POLITECNICO DI TORINO

Corso di Laurea Magistrale
in Ingegneria Biomedica

Tesi di Laurea Magistrale

Curcumin-mediated synthesis of magnetite and gold nanoparticles for biomedical applications

Relatori
prof.ssa Enrica Verné
prof.ssa Marta Miola

Candidato
Arianna Galatà

Anno Accademico 2020/2021

Table of Contents

SUMMARY 1

Introduction 5

Chapter 1 7

Multifunctional nanoparticles 7

1.1 Fe_3O_4-NPs and magnetic properties 10

1.1.1 Synthesis methods 11

1.1.2 Magnetic properties. 12

1.1.3 Biomedical applications. 17

1.2 Au-NPs and plasmonic properties 19

1.2.1 Synthesis methods 19

1.2.2 Plasmonic properties 20

1.2.3 Biomedical applications 21

1.3 Magneto-plasmonic NPs 23

Chapter 2 24

Green synthesis 24

2.1 Curcumin 31

2.1.1 Chemical characteristics of curcumin. 31

2.1.2 Curcumin biological activity. 33

2.1.3 Curcumin-metal ion interactions. 34

2.1.4 Curcumin delivery systems. 35

2.2 Curcumin-conjugated nanoparticles 36

2.2.1 Curcumin-magnetite nanoparticles. 36

2.2.2 Curcumin-gold nanoparticles. 38

Chapter 3 40

Materials and methods 40
3.1 Synthesis routes 40
3.1.1 Gold nanoparticles 40
3.1.2 Magnetite nanoparticles 42
3.1.3 Gold-magnetite nanostructures 45
3.2 Nanoparticles characterization 46
Chapter 4 49
Results and discussion 49
4.1 Curcumin 49
4.2 Gold nanoparticles 51
4.3 Magnetite nanoparticles 54
4.4 Gold-magnetite nanoparticles 59
Chapter 5 66
Conclusions 66
References 68

SUMMARY

1. Introduzione

Il crescente interesse verso le nanotecnologie ha condotto alla loro applicazione in svariati campi, tra cui quello delle scienze biomediche. La possibilità di sfruttare le proprietà magnetiche e ottiche dei materiali alla nanoscala ha permesso di utilizzare le nanostrutture sia in ambito diagnostico che terapeutico, inoltre, l'elevato rapporto tra superficie e volume delle nanoparticelle le rende ideali come vettori nelle applicazioni di rilascio mirato di farmaci.

L'obiettivo di questa tesi è lo sviluppo di una nanostruttura ibrida multifunzionale costituita da nanoparticelle di oro e di magnetite che vengono sintetizzate attraverso l'utilizzo innovativo della curcumina come molecola bioattiva.

2. Nanoparticelle multifunzionali

Il primo capitolo è costituito da una panoramica sulle nanotecnologie e le nanoparticelle multifunzionali, seguita da una trattazione sulle nanoparticelle di magnetite e di oro (che sono state sintetizzate durante il lavoro in laboratorio) ponendo l'attenzione sulle loro proprietà e sulle applicazioni in ambito biomedico.

Le nanoparticelle di ossido di ferro più diffuse per applicazioni biomedicali sono le nanoparticelle di magnetite, per via delle loro caratteristiche di biocompatibilità e stabilità colloidale ma soprattutto per la capacità di manifestare il fenomeno del superparamagnetismo. Le nanoparticelle con comportamento superparamagnetico non sono soggette ad isteresi per cui dopo la rimozione di un campo magnetico applicato dall'esterno perdono totalmente la magnetizzazione che era stata indotta. Di conseguenza, le nanoparticelle di magnetite sono considerate particolarmente adatte ad applicazioni quali l'ipertermia, il rilascio mirato di farmaci e l'imaging.

Le nanoparticelle di oro, oltre alla non tossicità, possiedono proprietà ottiche uniche: per via del fenomeno di risonanza plasmonica superficiale, esse sono in grado di emettere

calore se irraggiate a ben precise lunghezze d'onda. Questa loro proprietà viene sfruttata nella terapia fototermica, un trattamento antitumorale selettivo e minimamente invasivo. Inoltre, le nanoparticelle di oro sono possono essere impiegate in applicazioni di biosensing e rilascio mirato di farmaci.

3. Sintesi ecologiche

I metodi tradizionali di sintesi delle nanoparticelle sono costosi e dannosi per la sicurezza dell'uomo e dell'ambiente, di conseguenza negli ultimi anni molti ricercatori si sono concentrati sulla possibilità di sviluppare nuovi metodi di sintesi che possano essere ecologici e sicuri. L'utilizzo di piante o microorganismi come agenti bioattivi è una valida alternativa poiché essi sono in grado di ridurre gli ioni metallici attraverso gli enzimi e dei fitochimici che contengono, anche se i meccanismi di azione sono ancora sconosciuti.

La molecola bioattiva utilizzata per la sintesi delle nanoparticelle durante la fase sperimentale di questa tesi è la curcumina. La curcumina è un polifenolo derivato dalla curcuma comunemente utilizzata come spezia nel campo alimentare ma con potenzialità terapeutiche per via delle sue proprietà antiossidanti e antitumorali. I limiti all'utilizzo della curcumina derivano dalla scarsa biodisponibilità, dalla poca solubilità in acqua e dall'instabilità chimica, che però potrebbe essere superati grazie alla possibilità di integrarla nelle nanostrutture. Il secondo capitolo contiene un approfondimento sulle caratteristiche chimiche della curcumina e sugli studi pubblicati in letteratura inerenti alle nanoparticelle funzionalizzate con curcumina.

4. Materiali e metodi

Il lavoro sperimentale è stato condotto in tre fasi:

- sintesi delle nanoparticelle d'oro attraverso l'utilizzo della curcumina come agente riducente e stabilizzante;
- funzionalizzazione delle nanoparticelle di magnetite con biomolecole di curcumina;

- unione delle nanoparticelle di oro e magnetite attraverso la curcumina.

Prendendo spunto da lavori presenti in letteratura, sono state realizzate due sintesi di nanoparticelle d'oro che si sono differenziate fondamentalmente per il modo utilizzato nel disciogliere la curcumina: in un caso essa è stata disciolta in una soluzione acquosa di NaOH, nell'altro è stata aggiunta ad una soluzione di acqua bidistillata alla quale è stato poi aggiunto K_2CO_3 fino al raggiungimento di un pH entro l'intervallo di valori 9.2-9.6.

Anche per la funzionalizzazione delle nanoparticelle di magnetite sono stati provati due metodi differenti: nel primo, dopo essere state sintetizzate, le nanoparticelle sono state funzionalizzate con APTES prima di legare la curcumina; nel secondo si è cercato di ottenere la funzionalizzazione aggiungendo direttamente la curcumina durante il processo di sintesi delle magnetiti.

Infine, per cercare di raggiungere l'obiettivo di unire le nanoparticelle di oro e magnetite attraverso l'uso della curcumina, sono stati effettuati due tentativi: in un caso, il punto di partenza è stata la sintesi delle nanoparticelle d'oro seguita dal tentativo di legare le nanoparticelle di magnetite; nell'altro, le nanoparticelle di magnetite sono state funzionalizzate con APTES e curcumina che in seguito è stata utilizzata per ridurre l'oro direttamente sulla loro superficie.

Per la caratterizzazione chimico-fisica delle nanoparticelle sono state effettuate le seguenti analisi: le spettroscopie EDS e FT-IR hanno permesso di determinarne la composizione elementale e strutturale; il raggio idrodinamico e la distribuzione dimensionale sono stati ottenuti dall'analisi DLS; la spettroscopia UV-Vis è stata utilizzata per indagarne le proprietà ottiche.

5. Risultati

I risultati delle analisi di caratterizzazione effettuate sono stati riportati e discussi.

La prima sezione contiene lo spettro FT-IR della curcumina in polvere e gli spettri UV-Vis della curcumina disciolta nelle diverse soluzioni utilizzate durante le sintesi. I risultati ottenuti hanno permesso di determinare successivamente l'effettiva presenza della biomolecola sulle nanoparticelle.

L’azione riducente e stabilizzante della curcumina nei confronti delle nanoparticelle d’oro è stata confermata per entrambe le sintesi dalla presenza sugli spettri UV-Vis del caratteristico picco riferito al fenomeno di risonanza plasmonica superficiale.

Dall’analisi dei risultati si è evinto che la funzionalizzazione diretta delle nanoparticelle magnetiche con curcumina non è avvenuta, a differenza del caso in cui le nanoparticelle sono state precedentemente funzionalizzate con APTES che si è rivelato un metodo efficace.

Le analisi EDS hanno rivelato una presenza non significativa di oro nelle particelle sintetizzate con il primo metodo, la cui inefficacia è stata confermata anche dagli altri risultati. La riuscita del secondo metodo invece è stata confermata dalla presenza del picco dell’oro (seppur in piccole quantità) sullo spettro EDS e dalla presenza dei picchi della curcumina e della magnetite sullo spettro FT-IR.

6. Conclusioni

L’utilizzo della curcumina come biomolecola attiva che permetta di unire nanoparticelle di oro e di magnetite in un’unica nanostruttura ibrida appare promettente grazie ai risultati ottenuti con il secondo metodo di sintesi testato durante il lavoro sperimentale. Tuttavia, sono necessarie ulteriori analisi morfologiche per verificare l’effettiva riduzione delle nanoparticelle d’oro sulla superficie di quelle magnetiche.

Introduction

The advance of nanotechnologies represented a new frontier to explore in the scope of biomedical sciences. In particular, the interest of researchers focused on the development of multifunctional nanoplatforms due to the versatility of their properties that make them suitable for a theranostic approach. These structures at the nanoscale show enhanced magnetic and optical properties and can be remotely controlled which are optimal features since they are intended for use as contrast agents in imaging techniques and heat sources in hyperthermia treatment, as well as they can be employed as therapeutic agents for drug targeting and delivery because of their ability to carry large doses of drugs.

Nevertheless, the chemical and physical methods currently employed for the production of nanoparticles are costly and dangerous both for human health and the environment. Consequently, it is increased the amount of studies concerning the search for new synthesis methods that can be safe and eco-friendly focusing on the critical choice of the solvent medium and the reducing and capping agents. The use of plants and microorganisms as bioactive agents is an ecological alternative, as they are able to reduce metal through the action of their enzymes and active phytochemicals.

The aim of this thesis project is to develop an eco-friendly synthesis route involving curcumin biomolecule for the functionalization of magnetite nanoparticles and the reduction and stabilization of gold nanoparticles in order to produce a unique hybrid nanostructure owning both magnetic and optical properties. Curcumin is a polyphenolic component of turmeric, widely used as a food spice and with a therapeutic potential because of its antioxidant and antitumour properties; the limitations due to its chemical instability and low bioavailability can be overcome by loading curcumin on nanostructures with drug targeting functionality. Gold and magnetite nanoparticles have been selected as the component of these nanostructures because of their physico-chemical properties: the first are highly biocompatible and easy to synthesize, but their widespread application is mainly due to their ability to generate heat consequently to the irradiation at specified wavelengths; the latter are already used as contrast agents in magnetic resonance imaging but are also suitable for therapeutic applications because of

their superparamagnetic behaviour that make them easy to be remotely controlled, in addition to their low toxicity properties.

An overview on magnetite and gold nanoparticles is reported in the first chapter focusing on their properties and applications, followed by a study on the green synthesis methods which are becoming more and more popular. Then, the experimental work is presented describing in detail the synthesis routes tested to achieve the formation of curcumin functionalized gold magnetite nanostructures together with the characterization analysis performed to identify the obtained structure and composition. Finally, the obtained results are reported and discussed.

Chapter 1

Multifunctional nanoparticles

Nanoscience concerns the study of nanomaterials, which are structure at the nanometric scale 10^{-9}. Due to their small size, targeted methods are necessary to produce and work with nanomaterials. The *National Nanotechnology Initiative* defined nanotechnology as the manipulation of matter with at least one dimension sized from 1 to 100 nm. [1] Nanomaterials gained researchers attention because of the specific properties developed by a material at its nanometric scale: quantum size effect is not negligible at this scale and properties change as a function of the particle size, this explain the difference in terms of chemical, physical and biological behaviours between nanomaterials and their massive counterparts. [2][3] In nanomaterials, electrons energy levels are not continuous (as when compared to the bulk form) but discrete because of the confinement of the electronic wave function in up three physical dimensions. [3]

To date, several nanoparticles (NPs) (i.e. a material with equal nanoscale dimension with three external dimensions) have been produced and employed in different fields such as physics, optics, electronics and communication, energy, engineering, chemistry, material science, biology, and medicine. [2][4] NPs can present different shapes, various dimensions and can be formed from different materials, moreover, they can be classified in NPs that contain inorganic elements and the ones that are made of organic molecules. [2]

Among the *organic NPs* several examples can be listed:

- liposomes (50-100 nm), amphiphilic phospholipids vesicles with a bilayer membrane, that can be load with hydrophilic drugs within their aqueous interior and hydrophobic drugs dissolved into the membrane;
- dendrimers (<15 nm), synthetic polymers whose structure is constituted of a central core, branching units, and surface functional groups that make them excellent drug and imaging diagnosis agent carriers;
- carbon nanotubes (<100 nm), cylinders of coaxial graphite sheets with exceptional strength and electrical properties that behave as efficient heat conductors, because of their features they can be used as biosensors, drug carriers, and scaffolds.

Metals and metal oxides constitute the *inorganic NPs* that include:

- quantum dots, fluorescent semiconductor nanocrystals with size-tuneable optical properties, they are excellent contrast agents for bioimaging and labels for bioassays thanks to their high resistance to photobleaching and photo-chemical degradation;
- metallic NPs, characterized by their ability to express the localized surface plasmon resonance (SPR) phenomenon, consequently they result easily detectable with many techniques (for example optic absorption, fluorescence, electric conductivity) and suitable for bioimaging applications;
- magnetic NPs, spherical nanocrystals with superparamagnetic behave that can be used in magnetic resonance imaging (MRI), for hyperthermia treatment, and then for active targeting when their surface is functionalized, pure metals have excellent magnetic properties but are unsuitable for biomedical applications without proper treatment because of high toxicity and oxidative sensitivity. [5]

Surface coating with functional molecules and polymers is a fundamental step during NPs fabrication for many reasons: improvement of colloidal stability, enhancement of solubilisation and water-dispersibility, introduction of functional groups, properties modification and improvement and toxicity reduction. [2][6]

Multifunctional NPs represent an emerging field because they provide a combination of two or more functionalities (such as magnetization, fluorescence, near-infrared absorption) within a sole system resulting in enhanced physicochemical properties, while monofunctional NPs are limited to a single effect. [2] As to produce multifunctional NPs different components have to be integrated into a unique system, it is necessary to pay special attention to the choice of the structures and the incorporating method, according to which multifunctional NPs can be classified as follows (Figure 1): polymer-NPs composites, constituted by functional polymers that encapsulate the NPs or are grafted on them; multiple inorganic NPs, that can be integrated forming core-shell, doped, or hetero structures; porous structure NPs, when the presence of porosity or hollow is crucial to obtain the functionalization. [7] For example, in biomedical field an application can be represented by the development of a unique multifunctional platform able for simultaneous targeting, imaging, and therapy administration.

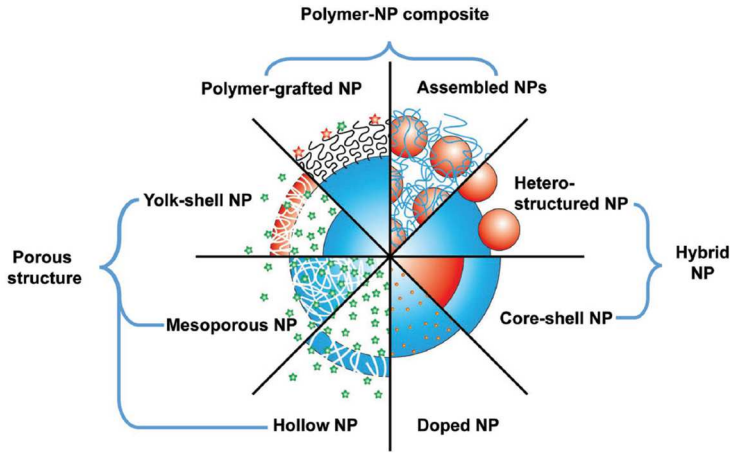

Figure 1. Structural classes of multifunctional NPs. [7]

Nanomedicine

Nanomedicine, which is the application of nanotechnology in the medical field, involves the development of new application in medical treatments, such as new imaging methods, faster diagnosis, drug/gene delivery and tissue regeneration, development of new medical products. [4] To date, some nanoparticles intended for use as theranostic agents (theranostics is a combined application of clinical diagnosis and therapy) are under clinical trials for human use.

There are several aspects that made the use of NPs in medicine a fascinating perspective over the years: their high surface-volume ratio, the tunability of their properties, and most of all their ability to work at cellular and molecular level since they own the same size range of lots of biomolecules (such as proteins, antibodies, nucleic acids). In biomedical applications, surface coating is essential to avoid the formation of agglomerates or precipitation and mostly to improve the colloidal stability of NPs, that allows to prolong their blood circulation time before the recognition by the reticulo-endothelial system. [3][6] The half-life of drug clearance in tissues can also be regulated through the choice of NPs size: it must be small enough (<200 nm) to avoid short blood circulation time caused by prompt splenic and liver filtration, and large enough (>10 nm) to evade kidney filtration and rapid penetration.

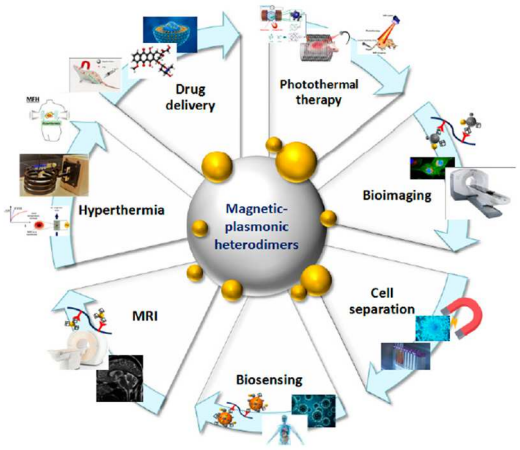

Figure 2. Potential biomedical applications of magneto-plasmonic NPs. [8]

1.1 Fe_3O_4-NPs and magnetic properties

Iron oxide nanoparticles (IONs), especially magnetite (Fe_3O_4) and maghemite (γ-Fe_2O_3), are the most widely used and promising structures for biomedical applications, because they present superparamagnetism that is a very useful and attractive property since these nanomaterials can be directed to active site by using an external alternating current (AC) magnetic field. [9]

The IONs physicochemical properties differ according to their iron oxidation states. *Magnetite*, a ferromagnetic black colour iron oxide of both Fe(II) and Fe(III), is the most popular one because of the Fe^{2+} state that can act as an electron donor. [10]

Iron oxide magnetic particles can be divided into three classes based on size: micron-sized iron oxide particles (MPIO); superparamagnetic iron oxide (SPIO), whose hydrodynamic diameter is larger than 50 nm; ultrasmall superparamagnetic iron oxide (USPIO), whose hydrodynamic diameter is lower than 50 nm. [9] SPIONs are particularly interesting because in addition to superparamagnetism they own features like biocompatibility, biodegradability, and ease of synthesis. [10]

Generally magnetic NPs are employed in the form of colloidal suspensions called ferrofluids (or magnetofluids). *Ferrofluids* consists of a liquid phase which contains uniformly distributed IONs (at a concentration of 10^{21}-10^{23} particles/m^3) functionalized with surfactants to enhance stabilization. The possibility to combine fluidity and

interaction with an external magnetic field is considered the main advantage of using ferrofluids in biomedical field. [11][12]

Today studies address to improve IONs applicability by better developing and understanding their behaviour, that is strongly dependent from the fabrication conditions and surface functionalization. Fundamental characteristics of IONs to be used in biomedical applications are small size with narrow size distribution and high magnetization values joined to superparamagnetism. [6] A problematic related to these NPs is their intrinsic instability when stored over certain periods of time because they tend to agglomerate in order to reduce the energy associated with high surface to volume ratio. [13] When uncapped, these NPs are highly reactive and prone to easy oxidation under ambient conditions damaging in magnet behaviour and dispersion. [13] The main strategy to prevent agglomeration and oxidation is to coat them with layers of organic or inorganic stabilizing agents, this would prevent the degradation process during and after the synthesis procedures and allow to further functionalize the NPs increasing their biocompatibility for specific targeting. [13]

1.1.1 Synthesis methods [9], [13]–[15]

The synthesis of magnetic NPs permits to control their shape, stability, and dispersion trends. The IONs fabrication methods can be divided into three categories: *wet chemical preparation methods*, the most used and efficient in controlling particle size; *physical methods*, that convert molecular precursors to iron oxide nanostructures, though these do not control carefully the particle size; *microbial methods*, characterised by high yield, good reproducibility, good scalability, efficient control over the resulting particle size and composition.

Homogeneous solution precipitation is a classical for the lab-scale preparation of iron oxide magnetic NPs, routinely a precipitating agent is added to the aqueous solution of metal precursor generating an insoluble solid product. The advantages of this simple process are the high yields of the products and the dimensional uniformity of the particles.

A more suitable and widely used synthesis method is co-precipitation from aqueous solution containing Fe(II) and Fe(III) by adding an alkaline solution. Using this method, NPs size, shape and composition can be tailored by factors like the type of iron salts, Fe(II):Fe(III) ratio, reaction temperature, pH of the medium, volume and ionic strength of the solution.

Another approach to obtain magnetic NPs is thermal decomposition: generally organometallic precursors are decomposed in organic solvents using surfactants as capping agents under anaerobic conditions. This method supports better control of the dimension, shape and dispersion behaviours of the nanomaterials; unfortunately, reaction conditions (for example high temperature and use of toxic chemicals) can be related to safety issues.

Polyol method is a very promising liquid-phase approach to synthesize uniform IONs: under stirring and boiling conditions iron salts are suspended and reduced in multivalent alcohols solvent (the simplest representative of the polyol family is ethylene glycol); following the metallic precipitation, polyols can be easily removed by repeated washing. Beyond the excellent control of particle size and dispersity guaranteed by this method, a bigger advantage is the production of highly crystalline oxide NPs.

Microemulsion synthesis consists in mixing two immiscible solvents causing the formation of a thermodynamically stable isotropic dispersion (which is the microemulsion) with the presence of an interfacial layer of surfactant's molecule. With the use of simple equipment, this technique allows to synthesize a great variety of nanomaterials with excellent control over size, shape and composition, desired crystalline structure, and high specific surface area. If two identical water-in-oil microemulsions containing the desired reagents are mixed, the microdroplets formed will experience continuous collisions, coalescence and break again and again leading to the appearance of precipitate inside the micelles. At the end of the reaction, the precipitate can be extracted via filtration or by centrifugation. Unfortunately, this procedure is very efficient but also difficult to be applied at large scale because large quantities of solvents are necessary to produce considerable amounts of nanomaterials.

Hydrothermal (or solvothermal) route is one of the most successful methods to prepare magnetic NPs and ultrafine powders, despite higher temperatures and very high pressures are usually involved. The NPs size and size distribution can be controlled by precursors concentration and the duration of the reaction.

1.1.2 Magnetic properties.

Generally, any material can be considered as a magnetic one. Depending on the orientation of the magnetic dipoles constituent the materials when subjected to an external magnetic field, they are classified as:

- diamagnetic, that reject the magnetic field as weakly as they can generally be considered non-magnetic;
- paramagnetic, characterized by randomly aligned magnetic moments and zero net magnetization of the overall structure, the moments align when exposed to an external magnetic field generating a proportional magnetization in the same direction;
- ferromagnetic, whose magnetic dipoles are oriented parallel in absence of external magnetic field making them able to generate a spontaneous magnetization;
- antiferromagnetic, that have magnetic moments with an antiparallel alignment cancelling each other out and therefore leading to no magnetization;
- ferrimagnetic, which have magnetic moments with an antiparallel alignment as antiferromagnets but with different magnetization values in the two orientations, resulting in a spontaneous magnetization. [15]

Magnetic activity is strongly dependent on material size and temperature and on the applied magnetic field, in fact magnetite nanoparticles (MNPs) exhibit superparamagnetism while bulk magnetite has a ferrimagnetic behaviour. [16] In massive ferromagnets, there are several uniformly magnetized regions (called magnetic domains) separated by non-uniform magnetization distributions; the net magnetization is low because of the non-aligned magnetization vectors of each domain. [10] Because of the finite-size effects resulting from the quantum confinement of electrons, the *superparamagnetism phenomenon* generally occurs in NPs with dimension <20 nm. As the particle size of the magnetic material decreases below the single magnetic domain, they exhibit higher magnetic susceptibility.

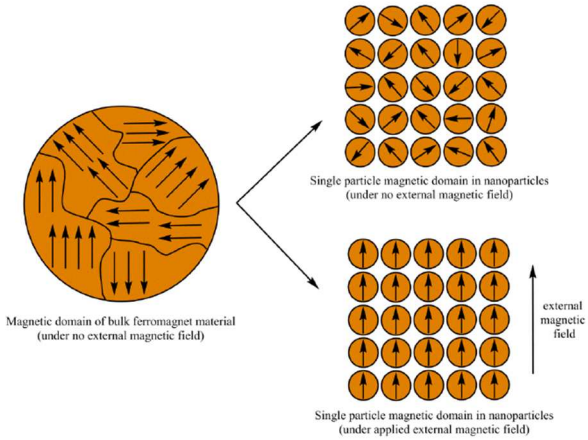

Figure 3. Schematic representation of magnetic ordering in bulk ferromagnet material and single particle domain. [16]

Superparamagnetic NPs become magnetized up to their saturation level but no hysteresis is produced, so the removal of the external magnetic field produces the total loss of their magnetization; this is a fundamental property for biomedical applications that concur to avoid coagulation and the possibility of agglomeration in vivo. [6][10][14] Referring to the H/M diagram (where H is the applied magnetic field and M is the magnetic induction) in figure 4, it is possible to define some significant magnetic parameters: the *saturation magnetization* (M_s), the maximum magnetization value achieved when the applied magnetic field causes the alignment with itself of the material magnetic dipoles; the *remanent magnetization* (M_r), the magnetization value after the removal of the applied magnetic field; the *coercivity* (H_c), the magnitude of the field that must be applied in the opposite direction to bring the material magnetization to zero.

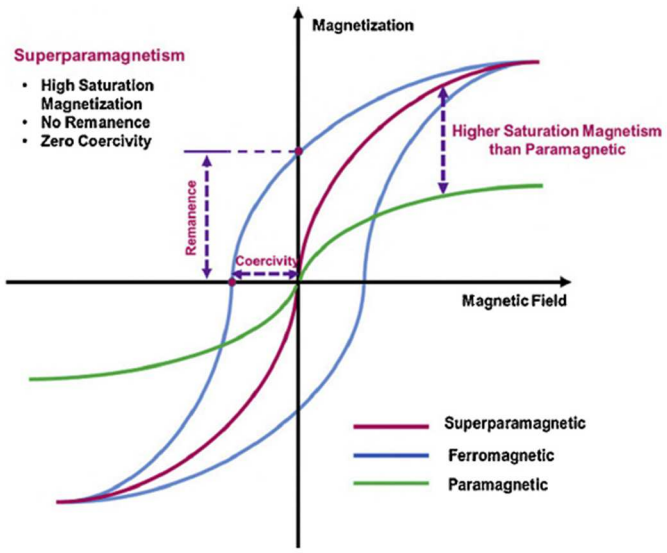

Figure 4. Magnetization characteristics of ferromagnetic materials. [10]

After the external field removal, the residual magnetization loss is a non-equilibrium process occurring with one or a combination of two relaxation mechanisms. The rotation of the particles' magnetic moment needs to overcome an energy barrier in order to align to an applied magnetic field, for uniaxial particles this energy is directly proportional to the magnetic anisotropy K and the particle volume V. The mechanism of the magnetic dipole rotating within the particle is called *Néel relaxation* and is described by the relaxation time:

$$\tau_N = \tau_0 e^{\frac{KV}{kT}}$$

Where τ_N is the Néel relaxation time, τ_0 ($\sim 10^{-9}$ s) is the characteristic flipping time, K*V is the anisotropy energy, k is the Boltzmann constant, and T is the temperature. Another relaxation mechanism named *Brownian relaxation* may arise in ferrofluids because of the particles ability to freely rotate in magnetic suspension, and the characteristic relaxation time can be modelled as:

$$\tau_B = \tau_0 \frac{3\eta V_h}{kT}$$

Where τ_B is the Brownian relaxation time, η is the viscosity of the carrier fluid, and V_h is the hydrodynamic volume of the particle. The effective relaxation time can be assumed as:

$$\frac{1}{\tau_{eff}} = \frac{1}{\tau_N} + \frac{1}{\tau_B}$$

It is noticeable the predominance of the faster relaxation mechanism. The delay in the rotation of the magnetic moments give rise to friction leading to a dissipation of energy in the form of heat. It is possible to estimate the heat dissipation value P with the following equation:

$$P(f, H) = \mu_0 \pi f H^2 \chi''$$

Where μ_0 is the permeability of the free space (magnetic field constant), f is the frequency of the applied magnetic field, H^2 is the strength of the applied magnetic field, and χ'' is the susceptibility of the magnetic field (imaginary part). The energy produced by a nanoparticle in suspension in a viscous fluid can be calculated in terms of specific absorption speed (SAR) as:

$$SAR = 4.1868 \frac{P}{m_e} = C_e \frac{dT}{dt}$$

Where P is the power dissipated measured as the power absorbed by the sample under examination, m_e is the mass of the magnetic NPs, and C_e is the specific heat capacity of the sample. SAR calculation is used to evaluate the ability of the material to transform magnetic energy into heat and is the main parameter to determine the tissues heating. [5][17]

Magnetic properties can be influenced and optimized by some basic parameters of the magnetic NPs such as size, shape, composition, core-shell structure. The effect of particle size on the magnetic property is expressed by the following equation

$$r = \sqrt[3]{\frac{6k_b T}{K_u}}$$

where r is the particle radius, k_b is the Boltzmann constant, T is the temperature, and K_u is the anisotropy constant. There are two temperatures that influence the magnetic behaviour: the *Curie temperature* (T_C), that is the transition temperature to which a material loses its permanent magnetic properties; the *blocking temperature* (T_B), at which superparamagnetic ordering usually exists. [10]

In biomedical applications, magnetic properties can be exploited in different ways. For example, high saturation magnetization values and enhanced relaxation time of the protons in the surrounding environment are useful properties for biosensing and MRI applications, while the heating effect arising from Neel and Brownian relaxations is central in hyperthermia applications. [6]

1.1.3 Biomedical applications.

- **Hyperthermia**: hyperthermia, that can be a full-body or localized treatment, is a selective destruction of the tumour cells by remotely heating over the physiological temperature of 37°C in the range between 41-45°C. [10] The advantage of this treatment is that in this range temperature the normal cells damage is reversible unlike cancer cells, that are more heat sensitive because of the low concentration of oxygen and nutrients and the low pH in the tumour tissue; moreover, the tumour unorganized vasculature promotes the NPs accumulation. [18] Hyperthermia can also be combined with other cancerous treatments as radiotherapy and chemotherapy as it can enhance cytotoxicity of radiation and drug treatment. [19]

  In magnetic hyperthermia the temperature increase by applying a high frequency alternating magnetic field which allows SPIONs to release energy to the tissue in the form of heat followed by irradiation. An alternative is represented by magnetic fluid hyperthermia, that is the injection of a magnetic fluid within the tissue followed by the exposure to a low or moderate frequency alternating magnetic field. The Curie temperature represents an important feature for the magnetic nanoscale heaters, because they can prevent overheating acting as in vivo temperature control switches for $42<T_c<60$°C.

  It has been shown that magnetic hyperthermia treatment can induce tumour regression, for example breast cancer studies and clinical trials related to prostate cancer and other carcinoma have been performed. However, further

studies are required to optimize the delivery and the control over heat distribution. [6][10][14][18][19]

- **Drug delivery**: magnetic targeting consists of attaching drug molecules to magnetic NPs that can be injected and guided to a site of action under the influence of localized magnetic field-gradients till the completion of therapy.

  Drug delivery is an excellent tool to overcome the issues related to the administration via systemic blood circulation such as the toxic effect originating in healthy tissues and the necessity of high drug dosages because only a small quantitative is able to reach the tissue of interest. NPs can carry large doses of therapeutic agent and achieve high local concentration increasing the therapeutic effect at the desired site.

  The great advantage of using NPs with magnetic property is the possibility to target the organs to be treated, then natural environment conditions (pH, osmolality, etc) can be exploited for liberating the loaded drug. [14] There are different manners to load drugs on IONPs: inserting them in the polymer interspace of magnetic nanoclusters; chemically bonding them to the activated surface of the NPs; trapping them in the magnetoliposomes; encapsulating them in stimuli responsive polymer shell. [14][20]

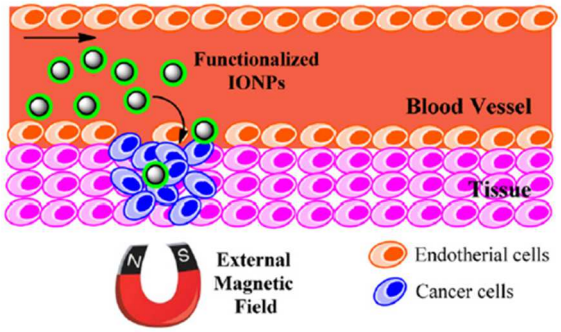

Figure 5. Schematic representation of magnetic nanoparticle-based drug delivery. [15]

- **Magnetic resonance imaging**: MRI is a non-invasive diagnostic technique with higher spatial resolution and contrast in soft tissues compared to other imaging techniques.

  During MRI a strong magnetic field (B_0) is applied leading water protons within the body tissues to align along it generating a precession motion around the direction of the field B0 at a certain frequency, named Larmor frequency. Then,

the protons are disturbed by a radiofrequency pulse at the Larmor frequency and align antiparallel to B_0, originating a transverse magnetization and decreasing the longitudinal one. Following the radiofrequency pulse removal, protons relax to their original state via two processes, the longitudinal relaxation (T_1) and the transverse relaxation (T_2). These processes are used to produce the image and there are two different imaging modes: T_1-weighted MRI image is the case of a shorter T_1 relaxation and a brighter contrast; T_2-weighted MRI image is the case of a shorter T_2 relaxation and a darker contrast.

Magnetic NPs can act as contrast agents making darker the MR image of the targeted area in contrast to the biological background, thanks to their high magnetic susceptibility that makes them able to shorten the transverse relaxation time in the site where are localized. [6]

1.2 Au-NPs and plasmonic properties

Gold nanoparticles (AuNPs) are considered very suitable for biomedical applications because of their nontoxicity, high biocompatibility, and unique optical properties; besides they are amongst the most stable metal NPs. All these features, in addition to the fact that they are easy to synthesize and functionalize, made possible their use as carrier systems and agents for photothermal therapy, as well as in biosensing and biodetection applications. [5][21] Normally, AuNPs are employed in the form of stable colloidal solution of cluster of gold atoms.

Converting bulk gold to NPs there is a colour change from yellow to ruby red accountable to the SPR theory (discussed later in detail). [16] As the SPR phenomenon originates from the way of AuNPs to interact with light radiation, they can be remotely controlled through laser irradiation with the aim to make them produce thermal energy when irradiated at specified wavelengths. [5]

1.2.1 Synthesis methods

Between the different chemical synthesis pathways for producing AuNPs, the most used is the *chemical reduction process*; other kinds of synthesis include thermal or photochemical reduction techniques, ionic liquids, electro deposition and physical methods like sonochemistry and radiolysis.

The chemical reduction synthesis can be divided into two fundamental steps: the *use of reduction agents* (like borohydrides, citric acid, hydrogen peroxide) which offer electrons to reduce the gold ions Au^{3+} and Au^{+} to Au^{0}, that is the electric state for NPs; the *use of stabilization agents* that prevent NPs aggregation by imputing a repulsive force that control NPs growth relatively to rate, geometric shape or final size, examples are surfactants, polymers, sulphur ligands. Sometimes the stabilizing agent can act as the reducing agent too. [3]

The AuNPs formation, size, and shape are strongly influenced by the chemical and physical characteristics of the synthesis, such as the ratio of gold to reducing agent, reaction temperature, pH, stirring rate. [3]

1.2.2 Plasmonic properties

The chemical, physical, and optical properties of metals are reliant on the spatial motion of the constituent electrons. Unlike the bulk materials, the dimensions much smaller than the wavelength of incident light (i.e., 1–100 nm) give rise to the confinement effect that is the spatial restrictions of electronic motion, leading to new properties in nanomaterials. [22]

The nanostructures of noble metals present the so-called *localized surface plasmon resonances* (LSPRs), that is collective oscillations of the conduction band electrons excited by an incident electromagnetic radiation on the nanoparticle at a specified frequency. The phenomenon frequency and intensity depend by the nanoparticle chemical composition, shape, and size, and by the dielectric environment where it is located. [23]

According to the Fermi liquid model, plasmons can be described as a negatively charged electron cloud coherently displaced from its equilibrium position around a lattice made of positively charged ions. Exposing to light metallic NPs, the oscillating electric field lead the free surface electrons to be excited and the local electron cloud to be asymmetrically distributed. The charge separation caused by the displacement of the electron cloud relative to the nuclei, is followed by Coulomb attraction between the negative electrons and the positive nuclei that produces a restoring force resulting into a series of back-and-forth oscillations of the electron cloud on the particle surface.

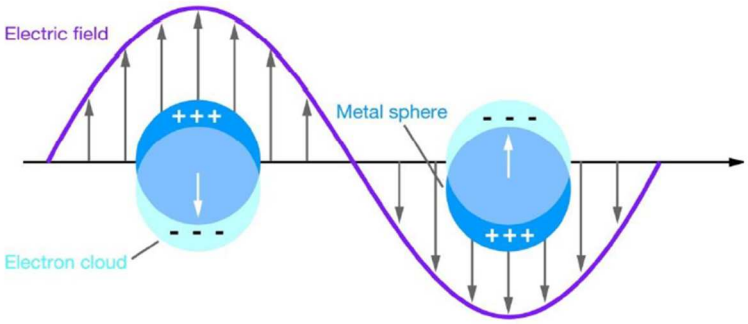

Figure 6. Schematic representation of a localized surface plasmon. [16]

The collective coherent oscillation of the conduction band electrons is called localized surface plasmon (LSP), because the plasmon oscillation is distributed over the entire particle volume. The matching of a particular incident light frequency with the LSP oscillation frequency of the plasmonic NPs is defined as the LSPR. [22] In absorbance measures of the nanostructures, the LSPRs manifest as narrow peaks in the spectral range going from the visible to the near infrared (at 520-550 nm in the case of nanospheres) because of the coupling between photons and conduction electrons of the NPs. Moreover, the peak is strongly correlated to the fact that LSPRs can generate phenomenon of local increasing of the electric field that can be further enhanced by controlling size, shape, and composition of the NPs and by exploiting their interactions. [23]

At the resonance condition, excited LSPs decay in two different manners: by *scattering*, that is radiatively by emitting photons at the incident light frequency; by *absorption*, that is non-radiatively by converting into hot electrons. The optical features (i.e. absorption, scattering, and extinction) of the plasmonic metal NPs are related to the wavelength of the light and to the size and shape of the NPs. For this reason, smaller NPs that act mostly as photo-absorbing agents are ideal for the photothermal effect-base biomedical applications, while lager NPs are preferred for biological imaging because of their scattering efficiency. [3]

1.2.3 Biomedical applications

- **Photothermal therapy (PTT)**: it is a minimally invasive selective cancer treatment, that make advantage of the large absorption band of nanomaterials in the near-infrared region (NIR) and the weak absorption by tissues.

  After the accumulation at targeted tumours, plasmonic NPs are stimulated with an external laser light and transform the absorbed radiation into thermal energy

causing a local temperature increase that induces the cancer cells apoptosis preserving the healthy tissues. [22]

Gold nanostructures represent an example of photothermal therapeutic agent as they can convert absorbed photons into thermal energy, causing cell destruction because of electron-phonon and phonon-phonon processes. [24] Despite the conventional dye molecules, AuNPs exhibit enhanced properties like higher absorption capacity, higher conversion efficiency of the absorbed radiation into heat, photostability, and biocompatibility. [5]

Being PTT a light-mediated treatment, the therapeutic efficiency is influenced by the choice of the external laser: NIR laser is the preferred one as it can penetrate deep into the tissues because of the low absorption or scattering exhibited by biological tissues as water, blood and fat. [22] However, radiation in the visible light region can also be used for in vitro studied and superficial tumour (as skin tumours).

PTT is a highly efficient disease treatment which exhibits several benefits: spatiotemporal selectivity, high sensitivity, side effects reduction, speed of treatment, low cost. [22] Moreover it has the great advantage to be performed by using light as external stimulus which is very helpful because is easy to focus, regulate and controlled. [5]

- **Biosensing**: AuNPs can be used for protein detections, because as substrates in Raman spectroscopy they can improve measurements of vibrational energies of chemical bonds. Also, they can be employed in dark-field microscopy for biological imaging application, thanks to their ability to produce an array of colours. [3]

  The features that make AuNPs suitable for these applications are the high scattering and the high photostability in comparison with other dyes, and the easy detection due to their strong emission power. [5]
- **Drug delivery**: gold nanocarriers are employed in targeted drug/gene delivery due to their tuneable optical properties. Besides conventional stimuli like temperature or pH, light modulation can be used for remotely trigger the release of drugs providing high spatiotemporal control. This behave permit to maximize drug efficacy by improving local drug accumulation while minimizing dosages and consequently unwanted side effects. [22]

To obtain targeting action AuNPs surface can be coated with hundreds of molecules (for example ligands, antibodies) thanks to the large ratio of surface area-volume and the presence of several binding sites. [3][5]

1.3 Magneto-plasmonic NPs

Among the various types of hybrid nanoparticle systems, the following work focuses on gold-magnetite NPs. The combination of Fe_3O_4-NPs with AuNPs leads to the formation of a unique nanostructure which exhibit both optical and magnetic enhanced properties, as well as overcoming the disadvantages of the single structures.

Relatively to AuNPs, only a small fraction manages to bind with tissues and their circulation time in the bloodstream is short because they are quickly excreted by the liver and kidneys; these reasons make them unsuitable for applications like MRI contrast agents. On the other hand, iron oxide tendency to oxidation causes instability issues and a polymeric or organic coating is essential for MNPs colloidal suspension. Also, they cannot attach a great variety of biomolecules.

Moreover, there is a change in magneto-plasmonic NPs properties with respect to the individual structures. For example, the SPR absorption peak can be red shifted while magnetization saturation decreases and coercivity increases as reported by *Pariti* [16].

Coupled nanostructures can be realised with different morphologies, as core-shell, core-hollow shell, nanoflower, dumbbell shape, etc. [16] Several synthesis techniques have been explored, like co-reduction of mixed ions, seed-mediated growth, and organic phase temporary linker. The choice of the technique to use rely on the aim of the application, because the tailoring of synthesis parameters allows to get the desired nanostructure. [25]

Chapter 2

Green synthesis

The procedures for nanoparticles production are often hazardous and expensive, because of the high energy requested and the use of toxic precursors that lead to biological risks and the formation of environmentally pollutant coproducts. [26][27] To overcome these problems related to the conventional physical and chemical synthesis, in the last years a green approach to new synthesis methods have become the focus of researchers' studies. [26][27] The objective is to develop protocols for nanoparticles synthesis suitable for large scale production that are simple, single-step, clean, non-toxic, cost-effective, rapid, eco-friendly, biocompatible, and safe for clinical research. [27][28] Ecological synthesis can involve the use of biological products (like plant tissues, algae extracts, bacteria, fungi, and so on) that are able to absorb and accumulate the inorganic metal ions present around them. [26][27][28] During biosynthesis the dissolved metal ions are reduced into nanometals by the biochemical processes in biological agents, with a rapid rate of formation of metal nanoparticles compared to the chemical methods. [27][29] Some of the biogenic components possess a reducing, stabilizing and capping function, consequently external agents are not necessary; also, this favours the reduction in the number of steps necessary for other process such as the surface grafting of functional groups which make the nanoparticles biologically active. [27][29] The synthesis and its characteristics (like quantity and rate of production of nanoparticles) are influenced by some parameters that can be varied: ratio of metal salts and biogenic agents, temperature, pH, contact time, concentration of salt, concentration of extract depending on the species and the part utilised of the plant, micro-organisms, etc. [27][30] For example, low pH can causes the agglomeration of AuNPs and, consequently, a less number of nucleation. [27] It would be important to identify the stable systems able to produce nanoparticles with homogeneous size and morphologies. [27][30][31] A significant advantage deriving from this kind synthesis routes is the possibility to use the resulting nanoparticles in various applications and in particular in biomedical applications because of the achieved biocompatibility. In fact, the green synthesis differ from the chemical one for the absence of toxic contamination caused by

products grafted to the nanoparticles that can limit their use. [27][28] However, though the resulting nanoparticles are coated with different types of biomolecules, their physico-chemical characteristics are not always suitable for use in biological studies. [26][31]

The biogenic agents can reduce the metal ions leading to the synthesis of metal nanoparticles because of the presence of different chemical entities, but the mechanism of synthesis is still unidentified even if some hypothesis have been proposed. [27][30] The plant extracts contain biomolecules involved in the reduction and capping of the nanoparticles, a phenomenon that is environmentally benign as well as chemically complex; examples of biomolecules are: polysaccharides, amino acids, proteins, vitamins, enzymes, flavonoids, phenolic acids, polyphenols, organic acids, alkaloids, terpenoids. [27][28] Instead, reductases, naphthoquinones, anthraquinones, and flavonoids are the compounds with a redox potential which allows them to play a role in the micro-organisms mediated biosynthesis. [27][29]

Nanoparticles biosynthesis by using plants extract

Plants have the capacity to hyper-accumulate, biologically reduce, and stabilize metal ions thanks to the active biomolecules present in their extract; the different composition and concentration of these substances in plants and their interaction with aqueous metal ions highly influence the size and shape of the resulting nanoparticles. [28][31] In biosynthesis approach several plant parts can be used, as stem, leaf, fruit, bark, peel, root, flower, etc. Before using them, it is necessary to obtain an extract of the plant tissue by washing with distilled water, cutting into small pieces and boiling in distilled water; also, it is possible to further purify the extract by methods like filtration and centrifugation. [27] The biosynthesis procedure consists of mixing the metal salts solution with the plants extract (generally at room temperature), then the reaction of biochemical reduction that lead to the formation of nanoparticles occurs within minutes; so this can be considered a one pot and single step method. [27][28] In order to be collected for further use, the nanoparticles are centrifuged at high speed and washed thoroughly. [27] The synthesis process takes place in various steps: an initial activation period, when the metal ions oxidation state changes from mono or divalent to zerovalent state and the reduced metal atoms nucleate; a growth period, when smaller neighbouring nanoparticles assemble in larger nanoparticles to reach a more stable thermodynamic

condition up to form different morphologies (spheres, triangles, rods, and so on), meanwhile further biological reduction of metal ions occurs; a final period, when the most energetically stable morphology of the nanoparticles is achieved thanks to the stabilization mediated by the biomolecules. [28]

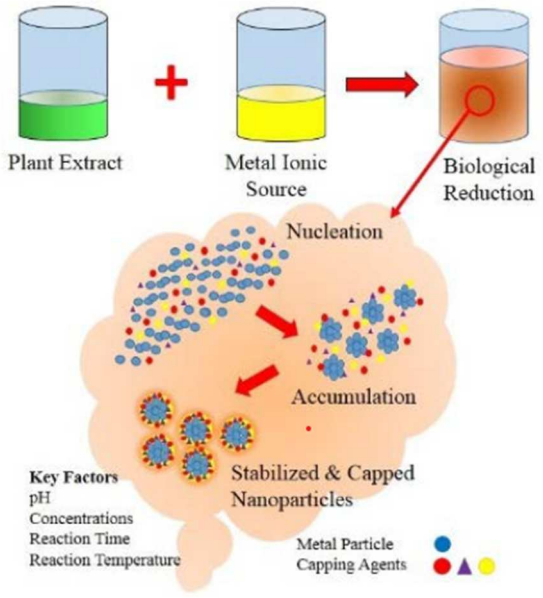

Figure 7. Biological synthesis of nanoparticles using plant extracts. [28]

A huge amount of studies is present in literature as lots of different plants have been employed as biological agents in the synthesis of metal nanoparticles. The following table lists just a few of them including some information, like type and size of the nanoparticles and active biomolecules involved in the reaction process.

Table 1. Biosynthesis of nanoparticles using different plants as bioreductants.

Plant	**Nanoparticle**	Additional Information	**Ref.**
Turmeric extract	Fe_3O_4	The synthesized spherical nanoparticles have a size of 10-14 nm and good crystallinity. They are suitable for biomedical applications because of their characteristics of biocompatibility, that is non-cytotoxicity and non-genotoxicity and no-lysis induction of human red blood cells.	[26]

Syzygium cumini seed extract	Fe_3O_4	This extract can act as green solvent, reducing and capping agent due to the presence of sodium acetate that has an electrostatic stabilizing function.	[32]
Carob leaf extract	Fe_3O_4	The synthesized nanoparticles have a size of 4-8 nm and result well monodisperse. Protein within the extract act as capping agent due to their carboxylic groups.	[33]
Syzygium cumini fruit extract	Ag	The mechanisms of reduction and stabilization of the nanoparticles involve the flavonoids that take part in the redox reaction.	[34]
Syzygium aromaticum buds extract	Au	The nanoparticles are reduced by the flavonoid compounds present in the extract.	[35]
Grape seed, skin, and stalk	Au	The synthesis lead to the formation of 20-25 nm sized nanoparticles. The reduction into gold atoms is mediated by catechin (i.e. a single basic monomer molecule), that also surround the nanoparticles creating a catechin-Au complex.	[36]
Hovenia dulcis fruit extract	Au	The extract is made of bioactive molecules, among which especially flavanol derivatives can bind with gold ions and reduce them with their hydroxyl and carbonyl groups.	[37]
Lonicera japonica flower extract	Au	The reduction and stabilization of nanoparticles involve different functional groups: amide, alkane, amino, and alcohols. The resultant nanoparticles have an antimicrobial activity.	[38]
Erigeron annuus flower extract	Au, Ag	It is used as reducing and capping agent and lead to the production of gold nanoparticles of 20-50 nm.	[39]

Lemongrass extract	Au-Ag	It is used for the synthesis of triangular shaped Au core-Ag shell nanoparticles. The potential mechanism consists of the gold nanoparticles reduction by electrostatic complexation with negatively charged lemongrass, after that ascorbic acid reduces the surface-bound Ag^{+}.	[40]
Terminalia arjuna leaf extract	Au	The nanoparticles reduction is mediated by different biomolecules: arjunetin, leucoanthocyanidins, hydrolysable tannins. The obtained nanoparticles have a size of 20-50 nm.	[41]
Neem leaf broth	Au, Ag, Au-Ag	The reduction of pure metallic and bimetallic nanoparticles is mediated by sugars and terpenoids, while flavanone and terpenoid act as surface active biomolecules inducing the stabilization of the nanoparticles.	[42]

Nanoparticles biosynthesis via microbial agents

Unicellular and multicellular microorganisms can synthesize inorganic materials through a bottom-up approach, as their secreted biomolecules (enzymes, proteins, sugars, etc.) lead to the formation of nanoparticles by the reduction/oxidation of metallic ions. However, the various types of microorganisms have different behaviours and way of interaction depending on the metallic ions; for this reason, further studies are required for a better comprehension of the synthesis mechanisms. [28] In addition to the ordinary environmental factors as temperature or pH, the biochemical processing activities of the microorganisms strongly affect the size and morphology of the synthesized nanoparticles. The main microbial routes for the synthesis of inorganic nanoparticles are mediated by: actinomycetes, algae, bacteria, fungi, viruses, yeasts. [28]

The nanoparticles biosynthesis mediated by micro-organisms can take place intracellularly or extracellularly. [27][28] Considering for example the AuNPs, in the first process Au^{3+} are absorbed and then reduced via unknown reactions, while in the latter micro-organisms alter environmental conditions after adding soluble Au^{3+} promoting the gold precipitation. [29] The extracellular method is particularly interesting as it allows to remove various synthesis steps. A sub-culture of micro-

organisms for 1-2 days is required before the biosynthesis, followed by the culture centrifugation to remove the biomass. The AuNPs bio-reduction occurs quickly after that supernatant are added to auric salt solution. At the end of the process, the AuNPs can be collected in the same manner as that obtained in plant extract-mediated synthesis. [27] In recent studies *Nangia et al.* reduced Au^{3+} to Au^{0} through a specific NADPH-dependent enzyme present in the isolated strain of *Stenotrophomonas maltophilia* bacteria and proposed a potential electron shuttling mechanism of synthesis whose schematic representation is reported in Figure 8. [43]

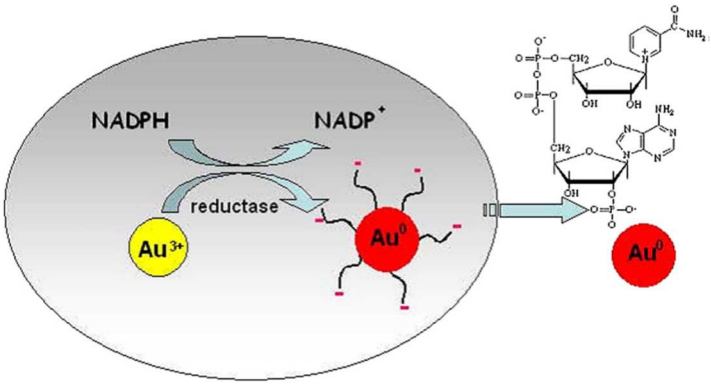

Figure 2. Proposed synthesis mechanism of GNPs by Stenotrophomonas maltophilia through enzymatic reduction. [43]

Active biomolecules

In literature it is also possible to find study concerning the action of biomolecules on reducing and functionalizing nanoparticles.

Wang et al. developed a one-step method for the synthesis of amino-functionalized MNPs using arginine, furthermore superparamagnetic manganese and cobalt ferrite nanoparticles can be obtained after slightly modifying the procedure. Arginine molecule has the function of alkali medium, stabilizer, and amino-functionalizing agent; in addition, its presence on the MNPs surface make them biocompatible and highly water dispersible. The process occurs at ambient conditions and $FeCl_2$ is the unique iron precursor utilized. The proposed formation mechanism consists of arginine-based chelation followed by reduction of the MNPs. [44]

Demir et al. involved maltose decomposition products and its acid in the synthesis of superparamagnetic iron oxide nanoparticles through a hydrothermal reduction route.

$FeCl_3 \cdot 6H_2O$ is the only iron precursor while glucose acts as reducing sugar and gluconic acid as capping agent. [45]

Apiin compound has been used as reducing and stabilizing agent by *Kasthuri et al*. in the novel synthesis route of gold and silver nanoparticles. The reduction of metal salt is carried out by the secondary hydroxyl and carbonyl groups of apiin, as shown in Figure 3. [46]

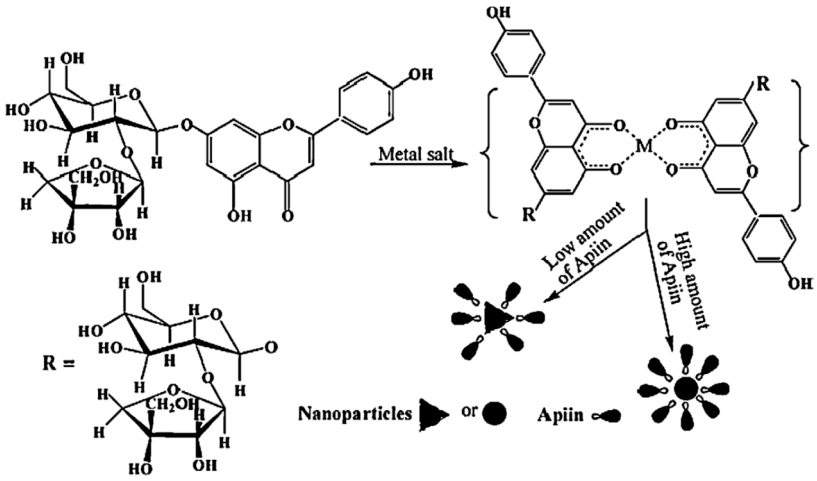

Figure 3. Schematic diagram of the formation of apiin-stabilized gold and silver nanoparticles. [46]

Wang et al. demonstrated that gallic acid, a polyphenolic compound, can be used as reducing agent in a one-step route for the synthesis of AuNPs; they also added PVP (i.e. a polymeric stabilizer) to improve the nanoparticles quality. The absorption of gallic acid on the nanoparticles surface is due to the presence of quinoid compounds with keto-enol functionality. [47]

2.1 Curcumin

Curcumin, also named diferuloylmethane, is a polyphenolic phytochemical compound consisting of a symmetric molecule (figure 4) made by a seven-carbon chain that link two aromatic rings at the ends derived from *Curcuma longa* (turmeric); it is mostly used as dietary supplement and spice, yellow pigment, and also herbal remedy. [48][49][50]

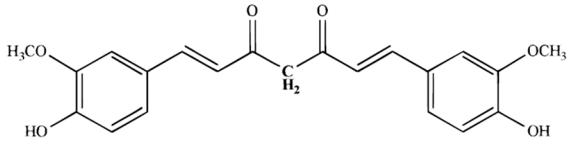

Figure 4. Curcumin molecule. [51]

The anti-inflammatory, antioxidant, antidiabetic, anticarcinogenic, antiparasitic, etc. properties and the possibility to use curcumin as chemopreventive, immuno-modulating, and therapeutic agent against several chronic diseases made it very attractive for researchers, but during the years the studies mainly focused on its biological activity despite the knowledge of its chemistry. [48][49][50] Curcumin is considered human safe since side effects did not occur after oral doses administration up to 8 g/days, moreover it is able to vary the activity of many drug-metabolizing enzymes through direct inhibition, induction, or down-regulation, leading to drug-drug interactions at the level of hepatic and intestinal metabolism. [49][50]

Curcumin can be extracted from turmeric or synthesized; the first method has been in use for the longest time, but both have been employed for more than a century to obtain curcumin. According to its origin and the soil conditions turmeric may contain from 2% to 9% curcuminoids (i.e. curcumin, demethoxycurcumin, bis-demethoxycurcumin, cyclic curcumin), where curcumin is the major component. The most popular methods are Soxhlet, ultrasonic, and microwave extractions, followed by column chromatography to separate curcumin from the mixture of curcuminoids. [48] The Pabon method is the simplest for the synthesis of curcumin through the reaction of 2,4-diketones with properly substituted aromatic aldehydes in the presence of boron trioxide, under anhydrous conditions and in a polar aprotic solvent. [48]

2.1.1 Chemical characteristics of curcumin.

Curcumin, whose IUPAC name is (1*E*,6*E*)-1,7-bis(4-hydroxy-3-methoxyphenyl)-1,6-heptadiene-3,5-dione, has a molecular weight of 368.38 g/mole (chemical formula

$C_{21}H_{20}O_6$) and a melting point of 183°C. [48][50] Pure curcumin is a crystalline material at room temperature and it is soluble in oil, acetone, dichloromethane, methanol, ethanol, and susceptible to pH variations in water: it is stable and insoluble in acidic and neutral conditions (the maximum stability is at pH=1.2) and become less and less stable and more soluble as pH increases. [50]

The predominant hydrophobic behaviour of curcumin (pH 2-7) is due to the presence of non-polar regions in the aliphatic chain, aromatic rings, and methyl group, but it became a hydrophilic substance (pH 8-12) after the deprotonation of the three hydroxyl groups that confer a negative charge to curcumin. [52] Its dissolution in aqueous systems is allowed by the presence of the phenolate ion, which is formed at neutral alkaline conditions after the hydrogen donation by the acidic phenol group that lead to the destruction of this structure; whilst, at acidic pH, the stability increases due to the conjugated diene structure as well as the aqueous solubility of curcumin decreases as the pH decreases because of the dissociation equilibrium that shifts towards the neutral form. [50]

Curcumin decomposition is pH and light dependent. [50] At the same environmental conditions the percentage of decomposed curcumin is much lower in absence of light, for this reason it is necessary to store curcumin correctly in order to avoid its photo-oxidation. [50] The crystalline curcumin can also be subjected to photodegradation, but it is more stable than the solubilized form. [52] Under neutral and basic conditions, when curcumin become chemically unstable, it undergoes hydrolytic degradation faster as compare to acidic conditions and give rise to five identified decomposition products: *trans*-6-(4'-hydroxy-3'-methoxyphenyl)-2,4-dioxo-5-hexenal is the major, while the others are vanillin, vanillic acid, ferulic aldehyde, and ferulic acid. [49]

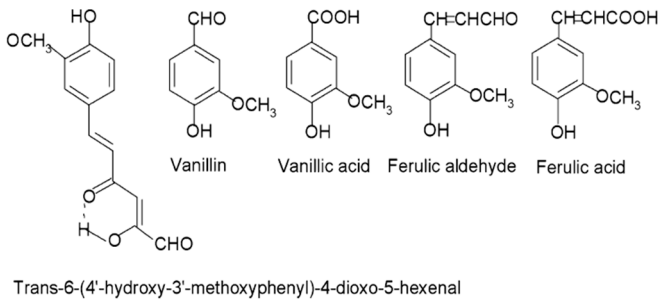

Figure 5. Chemical structures of curcumin decomposition products at pH 7.4. [49]

In the aromatic rings o-methoxy phenolic groups are present while the heptadiene link contains a bis-α,β-unsaturated β-diketone moiety that give rise to the keto-enol tautomerism of curcumin. [48][50] The physicochemical and antioxidant characteristics of curcumin rely on the keto-enol-enolate equilibrium of the heptadienone moiety. [51] In acidic and neutral aqueous solutions curcumin mostly exhibits the keto form (which is stable in the cell membrane), while above pH 8 the enolate form is the predominant one. [50][51] In the keto form, the heptadienone chain contains a highly activated carbon atom (the central one) with two labile hydrogens that became the site of reaction acting as a potent H-atom donor at pH 3-7, due to the delocalization of the unpaired electron on the adjacent oxygens which makes the C-H bonds very weak. [50][51] On the other hand, the phenolic part of curcumin is the reaction site in the enolate form and mainly act as an electron donor with a reaction mechanism analogue to the scavenging activity of phenolic antioxidants. [50]

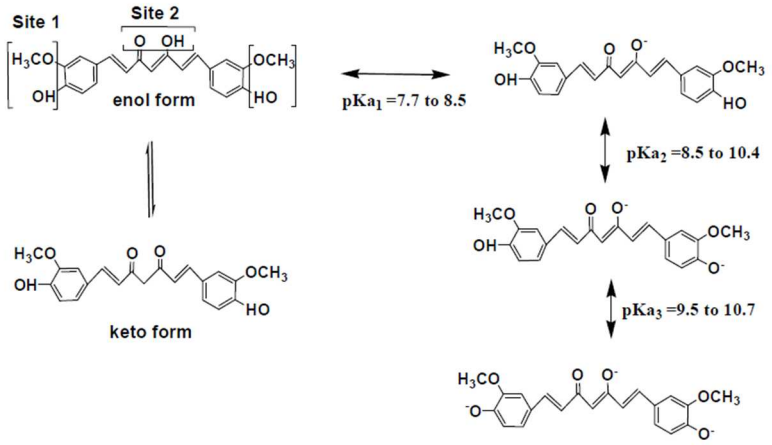

Figure 6. Curcumin in acidic and basic conditions. [50]

2.1.2 Curcumin biological activity.

The strong antioxidant activity of curcumin is helpful to protect cells from free radical-induced damage. Several chronic diseases (like inflammation, cancer, cardiovascular disease) are related to the reactive oxygen species (ROS) that interfere with the normal cellular function by the oxidation of proteins, lipids, and DNA biomolecules. The antioxidant activity of curcumin is due to its different action ability: free radical scavenger, chelating agent, singlet oxygen quencher. For example, curcumin is able to

chelate the iron ions preventing their pro-oxidant activity, or it can inhibit the action of lipid alkyl and lipid peroxyl radicals through is H-atom donor mechanism. [52][53]
Curcumin has a powerful anti-inflammatory activity because of its ability to suppress the inflammatory response enzymes and transcription factors, consequently inhibiting the production of inflammatory cytokines. Thereby, curcumin can be used for the treatment of the diseases caused by inflammation process (for example, the rheumatoid arthritis) and inhibit cancer formation thanks to this activity. [52][53]
It has also been reported that curcumin has an antimicrobial activity, as a consequence it can be used for the prevention or treatment of infectious disease. The potential mechanisms of action involve: the increase in bacterial cell membrane permeability; the inhibition of microtubule formation; the interference with key biochemical pathways; the damage of bacterial virulence factors. [52]
Curcumin can also prevent the growth of different tumour cells types because of its ability to inhibit angiogenesis and induce apoptosis. Studies have been carried out on prostate, colon, and breast cancer. [52]

2.1.3 Curcumin-metal ion interactions.

Curcumin is able to form strong complexes with several metal ions as the heptadienone moiety can act as chelating agent; generally, the curcumin:metal stoichiometry is 2:1 (Figure 7) but other ratios were also observed. The o-methoxy phenolic rings are not involved in the complex formation instead of the curcumin enolic group as the metal ion replace the enolic proton. In literature, examples of curcumin complexes synthesis with transition metals (Fe^{3+}, Cu^{2+}, Mn^{2+}, Zn^{2+}, Ni^{2+}, Cd^{2+}, Pb^{2+}, etc.), non-transition metal and rare earth ions (Al^{3+}, Ga^{3+}, Sm^{3+}, Y^{3+}, Se^{2+}, etc.), and metal oxides like VO^{2+}, have been reported. [48] The nature of the metal ion and the stoichiometry of the reaction conditions have an impact on the structure, physical properties and the stability of the curcumin-metal complexes; also, the biological reactivity of metals can vary due to their complexation with curcumin and their toxicity may be reduced. Some of these complexes can act as new metal-based antioxidants while others have a pro-oxidant activity. [48]

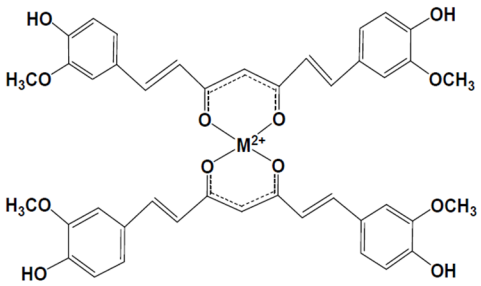

Figure 7. Structure of 2:1 curcumin:metal complex. [48]

2.1.4 Curcumin delivery systems.

The development of curcumin delivery systems, that can be organic or inorganic, is crucial to overcome the limitations due to the low water solubility, the chemical instability, and the low bioavailability of curcumin in cells. [48][52]

The most widespread solutions involving organic materials are the colloidal delivery systems, that is micelles, liposomes, emulsions, microemulsions, biopolymer particles, solid lipid nanoparticles, and nature-derived colloidal particles. All these kinds of formulations have advantages and disadvantages that make them more suitable for specific applications. [52]

Concerning the inorganic systems, some attempts have been made to bond curcumin with metal and oxide nanoparticles. Curcumin-loaded mesoporous silica nanoparticles (MSN) are systems that have attracted the researcher's interest because MSN can be easily functionalized and have been largely employed to improve the bioavailability of water insoluble drugs, furthermore they are biocompatible so can be used for biomedical applications. The conjugation of these nano systems is obtained through the oxygen of the curcumin diketo moiety that binds covalently with a silicon and lead to the enhancement of curcumin fluorescence. Curcumin can also be conjugated with cobalt and silver nanoparticles resulting in structures with antimicrobial activity. A deepening on the curcumin conjugation with gold and magnetite nanoparticles is presented in the following section. [48]

2.2 Curcumin-conjugated nanoparticles

The aim of the present work is the development of multifunctional nanostructures, constituted by magnetite and gold nanoparticles, to be synthesized using curcumin as bioactive agent. For this reason, in this section a research on already tested synthesis routes between the studies present in the literature have been conducted.

2.2.1 Curcumin-magnetite nanoparticles.

Only a few studies of curcumin-magnetite nanoconjugates are reported in the literature. Most of these concerns the possibility to load curcumin within biopolymer coated MNPs leading to the formation of nanostructures as the one represented in Figure 8. [48] Others describe methods to graft curcumin biomolecule after a pre-functionalization of the MNPs.

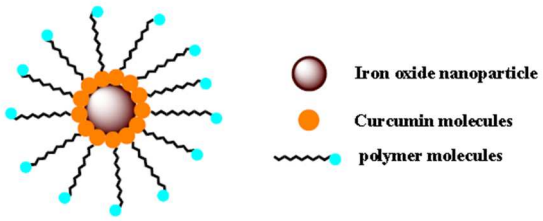

Figure 8. Polymer stabilized curcumin functionalized iron oxide magnetic nanoparticles. [48]

The details corresponding to some of these studies are reported in the table below (Table 2). Co-precipitation is the most used synthesis method, whilst the coating types and the way of loading curcumin are very varied.

Table 2. Examples of studies on curcumin-magnetite nanoparticles synthesis.

Synthesis method	Solution type	Coating	Cur-loading	pH	Ref.
Co-precipitation	Aqueous for NPs synthesis, different solvents tested for the Cur binding step	Citric acid or oleic acid	Through hydrogen-bond or -COOH functional groups	12-13	[54]

Co-precipitation	Aqueous	β-cyclodextrin + Pluronic F68 polymer	Diffusion e retention in hydrophobic cavity	-	[55]
Co-precipitation	Aqueous	-	Keto-enolic functionality of Cur molecule (acting also as stabilizer)	-	[56]
W/O microemulsion	Water in oil for NPs synthesis, aqueous for the chitosan binding step, ethanol for the Cur binding step	Chitosan	-	-	[57]
Solvothermal process	Organic solvent for NPs synthesis, aqueous for Cur binding step	DMSA (meso-2,3-dimercaptosuccinic acid)	Different tests on exposed functional groups	5.4 for Cur adsorption	[58]
Co-precipitation	Aqueous, ethanol for the Cur binding step	Chitosan or oleic acid	Adsorption	-	[59]
Co-precipitation	Aqueous	BSA (bovine serum albumin)	-	11	[60]

2.2.2 Curcumin-gold nanoparticles.

Curcumin-gold nanoparticles have been successfully synthesized and reported in some studies. The synthesis method is very simple and consists of mixing gold salts with alkaline curcumin solutions, so that the ionized curcumin can act as both reducing and capping agent since in this state not only the enolic -OH but the phenolic -OH too can donate hydrogen for the Au^{3+} reduction as shown in Figure 9. The curcumin-gold nanoconjugates are hemocompatible and non-toxic. [48]

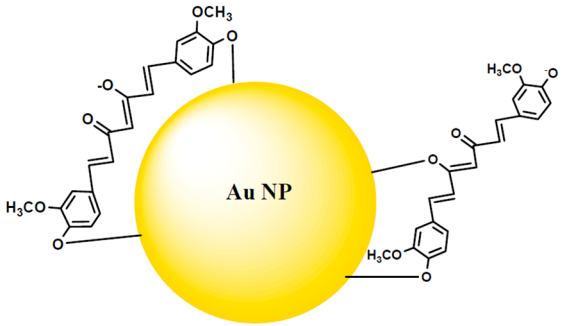

Figure 9. Gold nanoparticles capping by curcumin molecules. [48]

The following table (Table 3) contains the information about some examples of curcumin conjugated gold nanoparticles synthesis. Chemical reduction is the unique synthesis method employed while depending on the case curcumin may be dissolved in aqueous or organic solvent, it is always employed as both reducing and stabilizing agent; additional information is reported on pH and temperature synthesis parameters.

Table 3. Examples of studies on curcumin gold-nanoparticles synthesis.

Synthesis method	**Solution type**	**Curcumin action**	**pH**	**T**	**Ref.**
Chemical reduction	Aqueous	Reducing and stabilizing agent (metal chelation through the Cur diketone moiety)	-	T_{room}	[61]

Chemical reduction	Aqueous for $HAuCl_4$, organic (DMSO) for Cur	Reducing (Cur^{3-} formation consequently to the H-atom dissociation from the -OH group of the enolic Cur, O^- electrons reduce gold ions) and stabilizing agent	9.3 (Cur sol.)	-	[62]
Chemical reduction	Aqueous for $HAuCl_4$, organic (DMSO) for Cur	Reducing and stabilizing agent (O^- of the Cur molecule reduce gold ions while the unreacted aromatic rings and the heptadiene chain coat and stabilize the gold nanoparticle)	8-11	T_{room}	[63]
Chemical reduction	Aqueous	Reducing and stabilizing agent	-	-	[64]
Chemical reduction	Aqueous for $HAuCl_4$, organic (DMSO) for Cur	Reducing and stabilizing agent	9-10	-	[65]
Chemical reduction	Aqueous	Reducing (through the electrons transfer from Cur to gold ions) and stabilizing agent	5.67 (final)	90°C	[66]

Chapter 3

Materials and methods

The aim of this work is the development of a nanoplatforms containing both gold and magnetite nanoparticles generating a hybrid structure. One of the main challenges is to prepare the NPs through the use of curcumin biomolecule as novel biogenic agent with anti-inflammatory, antioxidant, antidiabetic, anticarcinogenic properties. In particular, this chapter contains a description of the synthesis methods tested during the experimental work and the techniques used to characterize the obtained nanoparticles in terms of physical, chemical and optical properties.

3.1 Synthesis routes

The experimental work performed to prepare the nanoparticles was conducted in three principal steps:

- Curcumin-mediated gold nanoparticles synthesis;
- Curcumin functionalization of magnetite nanoparticles;
- Conjunction of gold and magnetite nanoparticles using curcumin biomolecule.

Each of them is described in detail in the following paragraphs.

3.1.1 Gold nanoparticles

As the literature reports, several studies regarding the synthesis of AuNPs by involving curcumin in the process have been investigated [61]–[66], two different routes have been tested that differ for the way adopted to dissolve curcumin in water:

- in route 1 curcumin was dissolved in aqueous NaOH solution as proposed by *Sreelakshmi et al.* [61], as an highly alkaline environment promote the curcumin dissolution and OH moiety deprotonation;
- in route 2 curcumin was dissolved in bi-distilled water, then K_2CO_3 was used to obtain a pH value in the range 9.2-9.6, that *Sindhu et al.* [63] identified as the

ideal condition which lead to the formation of stable, spherical and crystalline nanoparticles.

AuNPs were synthesized by using the chemical reduction method with curcumin as reducing and stabilizing agent during both syntheses, the curcumin potential mechanism of action is shown in Figure 9. The deprotonation of its three hydroxyl groups is fundamental as the free electron on the oxygens reduce Au^{3+} to Au^{0} that subsequently nucleates and continue to growth forming nanoclusters, until these one reaches a size whose instability causes a cleavage phenomenon. At the end, after a maturation period, the final AuNPs are formed and stabilised by the aromatic rings and the heptadiene chain of the ionised curcumin that remain unaltered on their surface. [63]

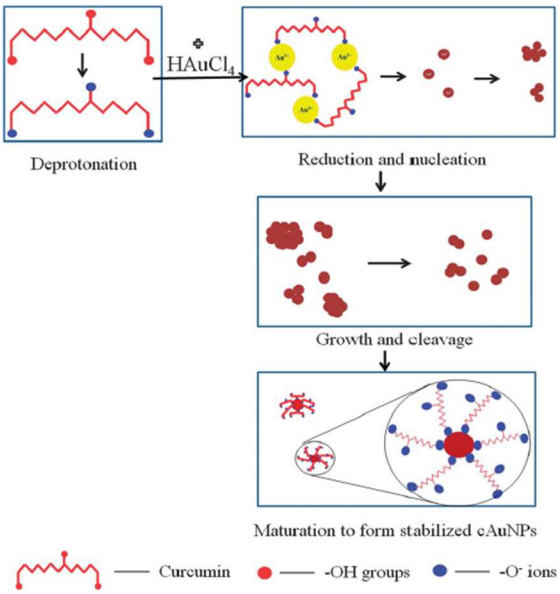

Figure 9. Mechanism of curcumin AuNPs formation. [63]

All the obtained nanoparticles solutions were stored in absence of light at low temperature.

Route 1

Firstly, a solution was prepared adding 0.02 ml of NaOH to 1.98 ml of bi-distilled water, the volume was made up to 10 ml with bi-distilled water; the solution had a pH value around 11.8. 3.68 mg of curcumin have been weighed and added to the solution

by causing a change in pH value (10.7) and in colour that turned red. To help curcumin dissolution, the suspension was left under magnetic stirring for a few minutes.
Finally, 1 ml of aqueous curcumin solution was mixed with 1 ml of 1 mM $HAuCl_4$ aqueous solution and allowed to stir for 2 hours.

Route 2

A solution was prepared dissolving 3.4 mg of $HAuCl_4$ in 10 ml of bi-distilled water.
1 mg of curcumin was dissolved in 10 ml of bi-distilled water obtaining a solution with pH=7.3. Then, 150 mM K_2CO_3 was prepared in bi-distilled water obtaining a solution with pH=11.7 to be used for buffering the pH of the aqueous curcumin solution in the range 9.2-9.6. The pH is a crucial parameter as the reduction of gold ions cannot occur at lower values because curcumin is insufficiently dissolved, whilst it is not stable at higher values leading to the precipitation of formed nanoparticles. [63] After adding dropwise the aqueous K_2CO_3 solution, the measured pH of the curcumin aqueous solution is 9.5.
Finally, the aqueous solutions of tetra-chloroauric acid and curcumin were mixed and allowed to stir and the nucleation of Au NPs.

3.1.2 Magnetite nanoparticles

On the basis of the scientific literature described in detail in the section "curcumin-conjugated nanoparticles" of the chapter 2, two different approaches have been conceived for the curcumin functionalization of MNPs:

- in route 1 MNPs were synthesized by a well-known process, that is co-precipitation of iron salts in aqueous medium, and functionalized firstly with (3-aminopropyl)triethoxysilane (APTES), then with curcumin;
- in route 2 curcumin was directly added during the magnetite synthesis process.

Route 1

Magnetite nanoparticles synthesis. The co-precipitation in aqueous medium of Fe2+ and Fe3+ salts was used for the synthesis of superparamagnetic iron oxide nanoparticles.
1.02 g of $FeCl_2 \cdot 4H_2O$ (0.1 M) and 1.3 g of $FeCl_2 \cdot 6H_2O$ (0.1 M) were dissolved in 50 ml of bi-distilled water in order to obtain two different 0.1 M solutions; each suspension have been stirred on magnetic plate to achieve the complete dissolution of the salts. Then, 37.5 ml of the aqueous $FeCl_2$ solution were added to 50 ml of aqueous $FeCl_3$

solution, the mixed solution had a pH=1.9. In order to induce the magnetite formation, the pH value was increased till the achievement of the range 9.5-10: NH_4OH was added dropwise to the solution keeping it under mechanical stirring, the reaction mixture turned black, indicating the formation of a suspension of iron oxide NPs. After that, the solution was sonicated for 20 minutes (SONICA® Ultrasonic Cleaner) and washed two times using bi-distilled water to remove the unreacted compounds. Finally, the MNPs have been resuspended in 100 ml of bi-distilled water, this final solution had a pH value of 8.5 and a nanoparticles concentration of 13,1 mg/ml.

Functionalization with APTES. The functionalization of the MNPs with APTES has the aim to enrich their surface with silanol groups that permit to easily bind curcumin, in addition to the advantage to stabilize nanoparticles in suspension. [67]
760 µl of the SPIONs suspension have been diluted in a solution of 1:1 bi-distilled water and ethanol for a final volume of 400 ml. In order to introduce terminal amino (-NH_2) groups on the particles surface the prepared suspension were mixed with a 20 ml of APTES (2% v/v) solution and stirred in thermal bath at 50°C for 24 hours. Afterwards, the solution has been washed two times with ethanol.

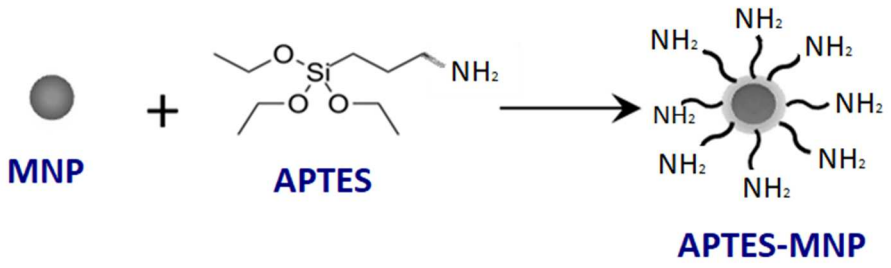

Figure 10. Schematic representation of APTES functionalized MNPs. [68]

Functionalization with curcumin. The APTES functionalized MNPs were resuspended in a solution made of 1 mg of curcumin dissolved in 10 ml of ethanol, then it was left under mechanical stirring for 3 hours. Finally, the solution has been washed two times with ethanol.
Sundar et al. hypothesized a reaction mechanism consisting on the APTES terminal NH_2 group binding with the OH of the curcumin phenolic moiety with the elimination of water; the schematic representation is reported in Figure 11. [67]

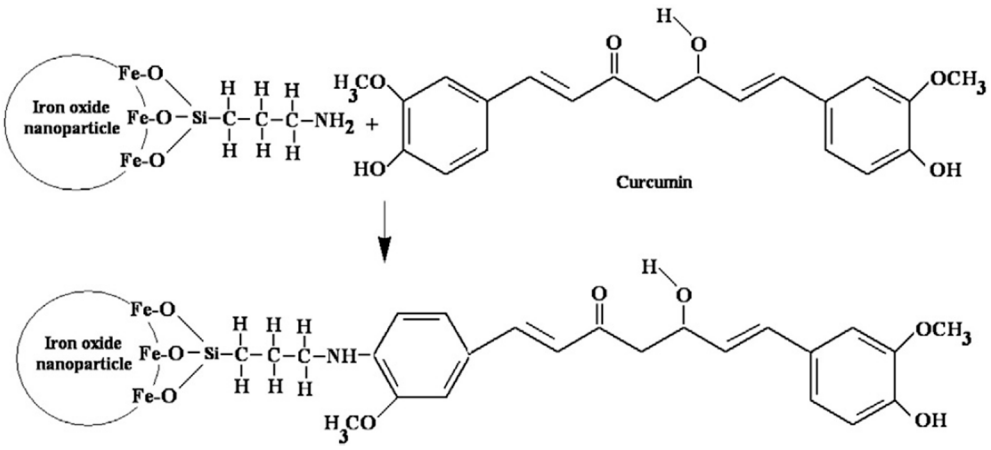

Figure 11. Curcumin binded on APTES coated MNPs. [67]

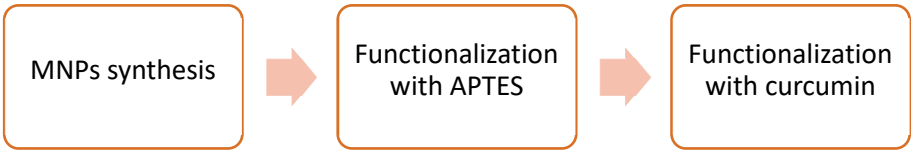

Route 2

Bhandari et al. [56] reported a method for the synthesis of curcumin functionalized MNPs, which was the inspiration for this route.

First, 10 mg of curcumin were dissolved in 10 ml of bi-distilled water.

The MNPs were synthesized by co-precipitation method as explained in "route 1" section introducing a new step and halving the amount of metal salts (0.51 g of $FeCl_2 \cdot 4H_2O$ and 0.65 g of $FeCl_2 \cdot 6H_2O$) while maintaining all the proportions to obtain 0.1 M solutions. Before dropping NH_4OH in the salt mixed solution (so, before the magnetite formation), the aqueous curcumin solution was added. Two different tests were conducted:

- the aqueous curcumin solution was added without modifications with a neutral pH;
- before adding the aqueous curcumin solution, the pH was adjusted by adding the aqueous K_2CO_3 solution (whose preparation is described in "gold nanoparticles-route 2" section) to reach a value of about 9.3.

These routes have been repeated varying the concentration of the iron salt solutions from 0.1 M to 0.01 M performing test 1, 2 and 3 as reported in the schematic representation below.

Test 1	Test 2	Test 3
• Iron salts solutions concentration 0.1 M • Aqueous curcumin solution at a neutral pH	• Iron salts solutions concentration 0.1 M • Aqueous curcumin solution at pH=9.3	• Iron salts solutions concentration 0.01 M • Aqueous curcumin solution at pH=9.3

3.1.3 Gold-magnetite nanostructures

As the aim of this work is the formation of hybrid nanostructures by using curcumin, consequently to the tests on curcumin mediated synthesis of gold and magnetite nanoparticles described in the previous sections two different routes have been tried out to achieve their conjunction:

- synthesis of curcumin AuNPs followed by the MNPs grafting;
- synthesis of curcumin functionalized MNPs followed by the reduction of AuNPs on their surface.

Route 1

19 ml of aqueous curcumin AuNPs solution have been synthesized via “gold nanoparticles-route 1” and mixed with 9.5 ml of the SPIONs solution obtained in the first step of “magnetite nanoparticles-route 1”, in order to have a 2:1 ratio. The mixed solution remained under stirring in thermal bath at room temperature for 30 minutes. After that, it was washed two times with bi-distilled water and resuspended in 20 ml of bi-distilled water.

This synthesis route was repeated one more time varying two parameters:

- the curcumin AuNPs were synthesized via “gold nanoparticles-route 2”;
- the gold:magnetite nanoparticles ratio was varied as 4:1.

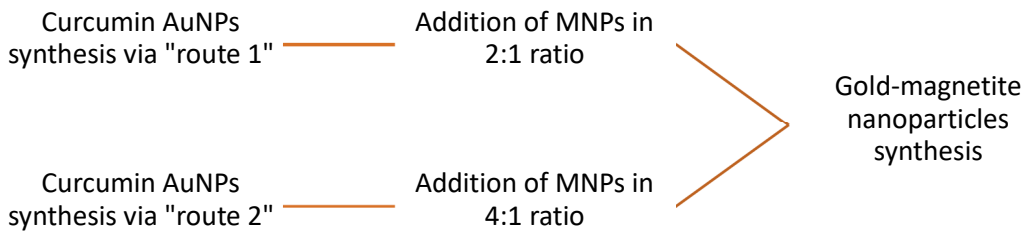

Route 2

The APTES-Fe_3O_4 nanoparticles have been functionalized with curcumin as described in "magnetite nanoparticles-route 1" except for final washes, that were made using bi-distilled water instead of ethanol, and they have been resuspended in 10 ml of bi-distilled water. 4 mg of $HAuCl_4$ were dissolved in 10 ml of bi-distilled water. The two aqueous solutions were mixed and left under mechanical stirring for 4 hours; then, the solution was washed two times with bi-distilled water.

3.2 Nanoparticles characterization

Characterization analyses have been conducted on the obtained nanoparticles as they are a crucial step to verify that the synthesis was successful and to investigate the chemical composition and optical properties of the nanoparticles. Various techniques have been used: ultraviolet-visible spectroscopy (UV-Vis), Fourier transform infrared spectroscopy (FT-IR), Dynamic Light Scattering (DLS), Energy Dispersive Spectroscopy (EDS).

Ultraviolet-visible Spectroscopy

This technique permits to determine the wavelength and maximum absorbance of compounds, for this reason it is widespread for the characterization of noble metals nanoparticles also providing information on their size and aggregation. The spectrometer contains a UV-Vis radiation source that emits a light, subsequently splitted by a monochromator to make only one wavelength pass through the sample and then be detected. The light intensity is converted by the detector in an electric signal and amplified. Finally, the absorbance is represented as a function of wavelength in a range that usually goes from 200 to 700 nm.

Nanoparticles samples are analysed as solutions, after being diluted in bi-distilled water that is used as reference for the measurement, and they are located in appropriate

cuvettes. UV-Vis (UV-2600 SHIMADZU) has been used to characterize gold and gold-magnetite nanoparticles.

Fourier Transform Infrared Spectroscopy

FT-IR spectroscopy is used to identify the organic functional groups present on the sample in order to obtain a structural and elemental characterization. When subjected to the IR radiation the specimen absorbs part of it, and the matter absorption and transmission can be reported on a spectrum. As chemical bonds vibrate at a characteristic frequency (depending on their structure, bond length, and angle), individual molecules that interact with the radiation absorb it at a specific wavelength. The different absorption peaks represented on the spectrum (ranging from 4000 to 450 cm^{-1}) refers to a specific chemical bond allowing to identify the individual compounds in a complex system.

The nanoparticles solutions have been dried in the incubator at 37°C until the complete evaporation of the solvent. Generally, samples have been used in the form of powder, except when the powder quantity was insufficient to perform the analysis; in this case, a tablet have been prepared using 198mg of KBr and 2mg of nanoparticles powder. FT-IR (JASCO 4000 Fourier transform infrared spectroscope) has been used to characterize magnetite and gold-magnetite nanoparticles.

Dynamic Light Scattering

DLS allows to determine particles hydrodynamic radius and size distribution. When the suspension is crossed by a laser beam, nanoparticles within it give rise to a light scattering phenomenon because of their Brownian motion that is influenced by their own dimensions. According to the scattering variations the diffusion coefficient is measured, while the hydrodynamic radius is derived through the Stokes-Einstein equation.

The nanoparticles samples have been diluted in bi-distilled water and located in appropriate cuvettes. The refractive index of AuNPs have been settled as 0.2773. DLS (Litesizer™ 500 instrument) has been used to characterize the AuNPs.

Energy Dispersive Spectroscopy

The EDS technique exploit the X-rays emission by the specimen to determine its elemental composition. As initially the sample's electrons are unexcited, a high-energy electron beam is focused on it and their interaction cause the excitement of an inner

electron with its displacement in a different energy level, leaving an energy gap. In this condition, the atom is excited so another electron from external shell has to occupy the vacancy to permit the atom's return to the ground state releasing an X-ray. The detection of the X-ray causes the ionization and the generation of an electrical charge that is measured. The X-ray energy (keV) is correlated with the distance between the two bands that is characteristic for each element resulting in exclusive picks in the X-ray spectrum that indicate the qualitative and quantitative chemical composition of the sample.

The spectroscope employed for the EDS measurement is a component of the FESEM (Zeiss supra 40 GEMINI x-ray spectroscope) instrument. The nanoparticles solutions to be analysed have been dried in the incubator at 37°C until the complete evaporation of the solvent, then the powder has been placed on a carbon grid. EDS has been used to characterize gold-magnetite nanoparticles.

Chapter 4

Results and discussion

In this section the results obtained during the experimental work are presented and discussed, also comparing them with the literature's results when appropriate. The first paragraph focuses on the characterization of curcumin biomolecule with the aim to better understand its behaviour in the conditions in which it was used, whilst the other paragraphs deal with the characterization of the gold, magnetite, and gold-magnetite nanoparticles synthesized.

4.1 Curcumin

The FT-IR spectrum of pure curcumin powder (**Errore. L'origine riferimento non è stata trovata.**) was detected to locate bands and peaks relative to the main functional groups, that are listed in the following table (Table 4).

Table 4. Functional groups of curcumin detected in FT-IR spectrum.

Functional group	Wavenumber (cm^{-1})	Ref.
C-O-C stretching vibrations	1027	[69]
Aromatic C-O stretching vibrations	1280	[69]
Olefinic C-H bending vibration	1430	[69]
Aromatic C=C vibrations	1510	[50][69]
C=O	1628	[50]
Phenolic OH stretching	3300-3500	[50][69]

The additional peaks of aldehyde at around 2845 cm^{-1} may be due to the presence of vanillin and feruloylmethane, that are curcumin degradation products.

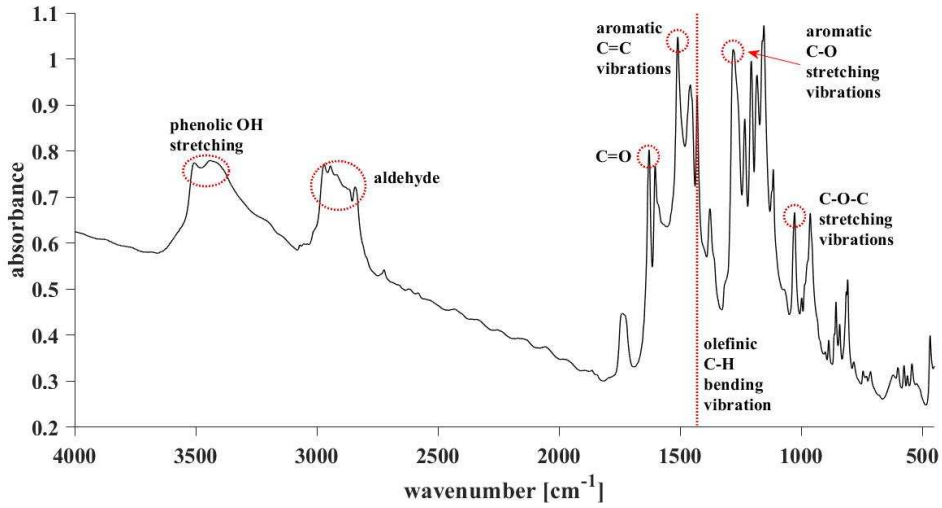

Figure 12. FT-IR spectrum of curcumin.

The UV-Vis spectrum of curcumin was detected for all the solutions in which it was dissolved to be used for the synthesis of nanoparticles, that are listed in Table 5 including information on pH and colour.

Table 5. Curcumin solutions employed for the nanoparticles' synthesis.

Solution	pH	Colour
Bi-distilled water	7.3	Colourless
Bi-distilled water + K_2CO_3	9.5	Orange-red
Bi-distilled water + NaOH	10.7	Intense red
Ethanol	-	Yellow

In Figure 13 it is possible to observe a strong peak at around 430 nm ([50][70]) and a smaller one at lower wavelengths (~250 nm [70]) both for curcumin dissolved in NaOH that for curcumin solution buffered with K_2CO_3; for curcumin dissolved in bi-distilled water instead, no peaks are detected since it is insoluble in acidic and neutral conditions.

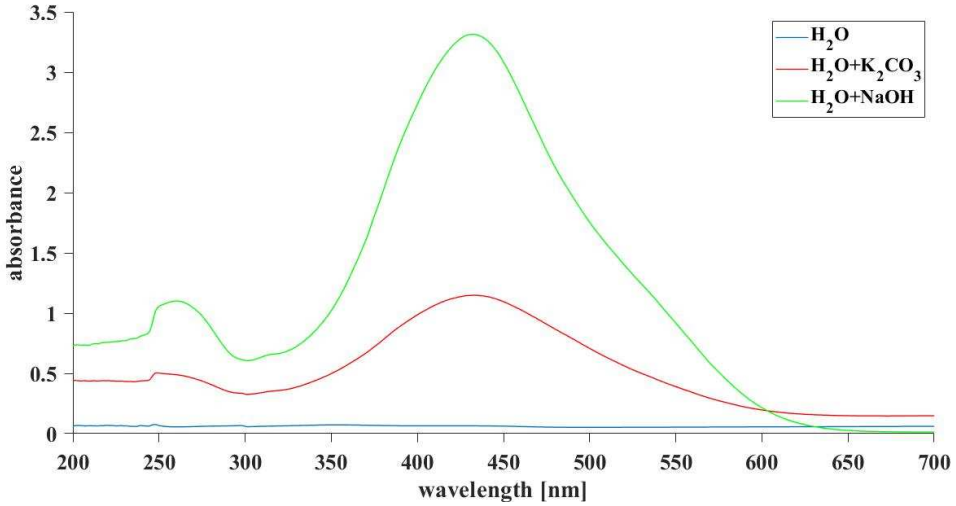

Figure 13. UV-Vis of curcumin dissolved in H_2O (blue), $H_2O+K_2CO_3$ (red), H_2O+NaOH (green).

Instead, in the UV-Vis spectrum of curcumin dissolved in ethanol (Figure 14) a broad band going from 360 to 500 nm is visible.

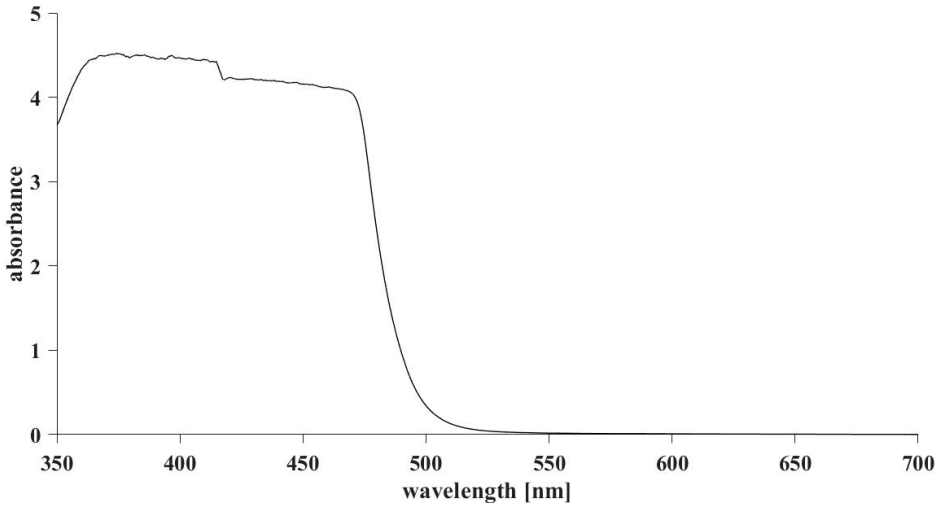

Figure 14. UV-Vis of curcumin dissolved in ethanol.

4.2 Gold nanoparticles

DLS. DLS analysis was performed to determine the hydrodynamic diameter (which is bigger than the real nanoparticle diameter as this value includes the electric dipole layer that adheres to its surface) and the polydispersity index (PDI, i.e. the breadth of the size

distribution) of the curcumin-gold nanoparticles synthesized via the two different routes, as using these parameters it is possible to characterize the physico-chemical behaviour of suspended nanoparticles. The measurements have been repeated three times so values are reported as "mean ± standard deviation" in Table 6.

Table 6. DLS results of curcumin gold nanoparticles.

	Hydrodynamic diameter	PDI
Route 1	**738.5±147.6 nm**	**46.43±0.058 %**
Route 2	**78.2±1.68 nm**	**22.9±0.001 %**

The average hydrodynamic diameter of the curcumin-gold nanoparticles obtained via route 2 is an order of magnitude lower than the ones obtained via route 1, as well as the PDI is halved indicating that this sample is more monodisperse than the other. However, the PDI value is much higher than expected in both cases so the presence of aggregates is hypothesized; this could be explained as the measurements have been carried out more than a month after the nanoparticles synthesis, which in the meantime have been stored at low temperatures and in absence of light.

UV-Vis. UV-Vis analysis has been used for the study of the synthesis routes of curcumin-gold nanoparticles because the observation of UV-Vis spectra allows to ascertain their formation when the characteristic SPR peak in the 500-600 nm band is present.

The UV-Vis spectrum of curcumin gold nanoparticles synthesized via "route 1" is shown in Figure 15. The SPR peak is clearly visible at around 540 nm, consequently the formation of the AuNPs and the ability of curcumin to act as reducing agent are confirmed. The peak that refers to curcumin shifted from 430 to 360 nm. [71] At the pH value of 10.7 all the three hydroxyl groups of curcumin are deprotonated and can be hypothesized as the reaction sites for the binding with gold ions, but *Sreelakshmi et al.* that developed a similar protocol indicated only the carbonyl group of enolic curcumin as the reaction site. [61]

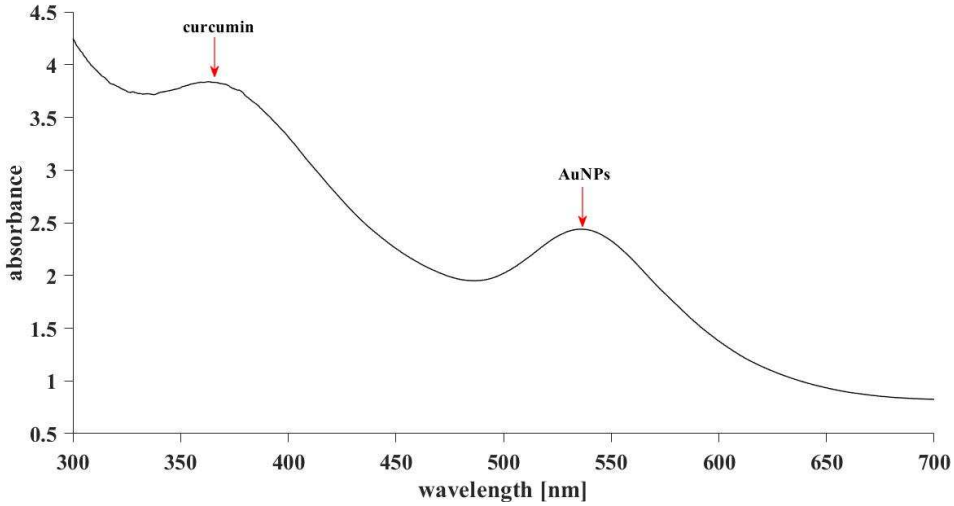

Figure 15. UV-Vis of curcumin-gold nanoparticles (route 1).

The synthesis of AuNPs is also achieved following "route 2" as their characteristic peak can be spotted at 540 nm in the UV-Vis spectrum (Figure 16) confirming again the reducing action of curcumin. Another peak is present at around 310 nm to be attributed to a displacement of the curcumin peak. In the work that inspired this synthesis attempt, *Sindhu et al.* deduced that after curcumin deprotonation all the three reaction sites (i.e. the two deprotonated oxygens of the aromatic rings and the one present in the enolic moiety) are involved in the reduction of Au^{3+} as described in chapter 3. [63]

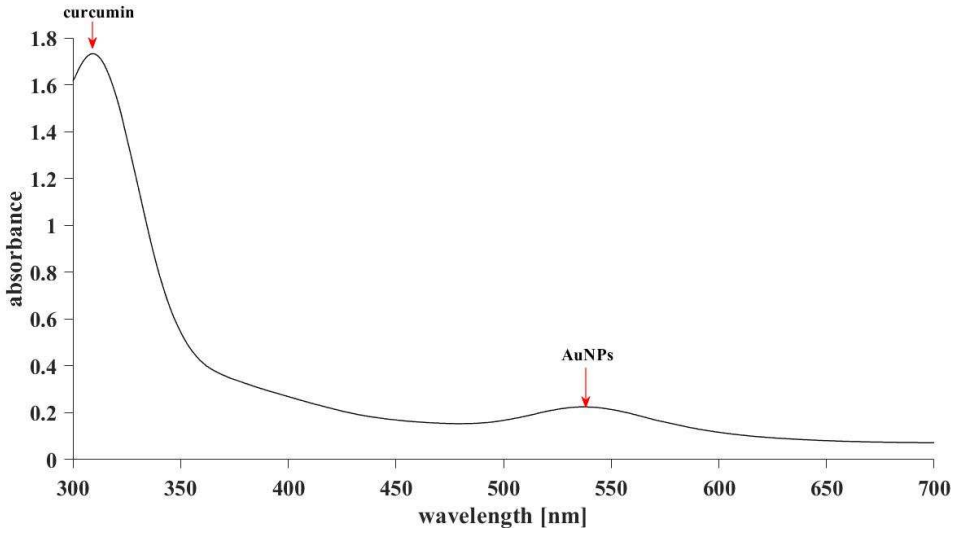

Figure 16. UV-Vis of curcumin-gold nanoparticles (route 2).

In both spectra the SPR absorbance peak is visible indicating the successful formation of AuNPs, although the one relating to "route 1" has a higher intensity in comparison to the corresponding peak that results after "route 2" synthesis this information cannot be

considered indicative as the absorbance value is correlated to the AuNPs concentration in the suspension, in fact afterwards the synthesis were repeated and the maximum absorbance values varied. Consequently, it can be assumed that these synthesis routes are strongly affected by environmental conditions as well as slight variation of pH or curcumin concentration, as stated in the previously cited studies too.

4.3 Magnetite nanoparticles

FT-IR spectroscopy was performed to verify the successful synthesis of MNPs and the correct grafting of curcumin and APTES molecules when employed.

Route 1. MNPs have been synthesized, then functionalized with APTES and later with curcumin, at the end of each step the FT-IR analysis was conducted.
The FT-IR spectra of MNPs and APTES functionalized MNPs are compared in Figure 17. The formation of MNPs is ascertained by the presence of a peak at 550 cm^{-1} that is characteristic of the strong vibrational modes of Fe-O bonds. The peak at 1000 cm^{-1} refers to the Si-O-Si vibrations in the silane layer confirming the successful functionalization of MNPs with APTES.

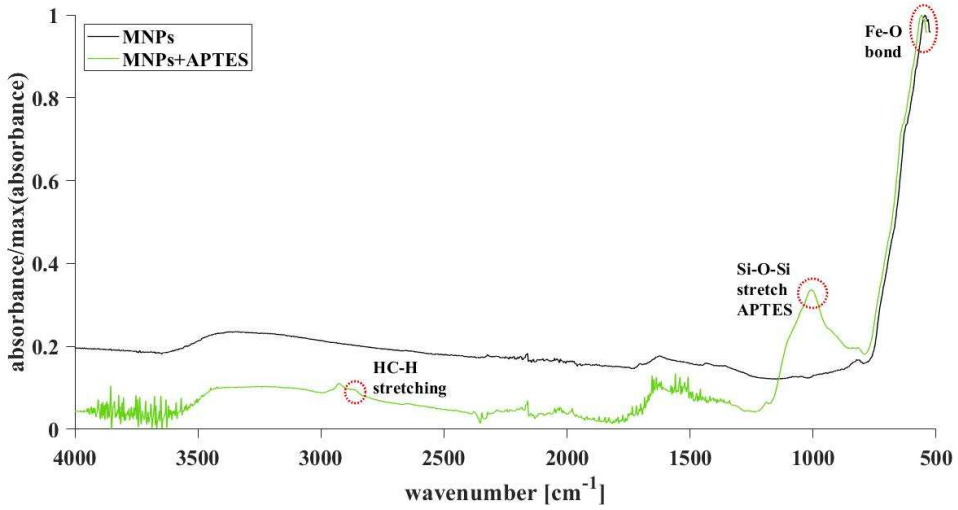

Figure 17. FT-IR spectra of magnetite nanoparticles (black) and APTES functionalized magnetite nanoparticles (green).

The further functionalization with curcumin can be confirmed by observing the spectrum in Figure 18 as the main signals of curcumin are present: at 1450 and 1500 cm^{-1} the peaks referred to the aromatic C=C bond, at 1635 cm^{-1} the peak related to the C=O bond, and at 3450 cm^{-1} the peak attributed to the stretching of the OH group of the phenolic moiety.

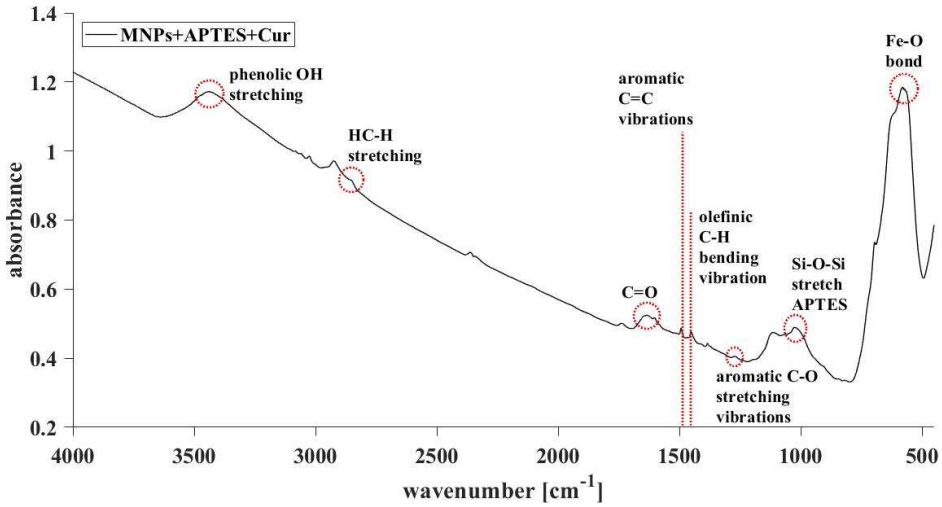

Figure 18. FT-IR spectrum of curcumin and APTES functionalized magnetite nanoparticles.

The UV-Vis analysis supports the hypothesis that the APTES-MNPs have been successfully functionalized with curcumin because of the presence of a peak at 440 nm (Figure 19). These results allow us to hypothesize the correct reaction between the APTES terminal NH_2 group and the OH of the phenolic moiety of curcumin, as described in detail in chapter 3.

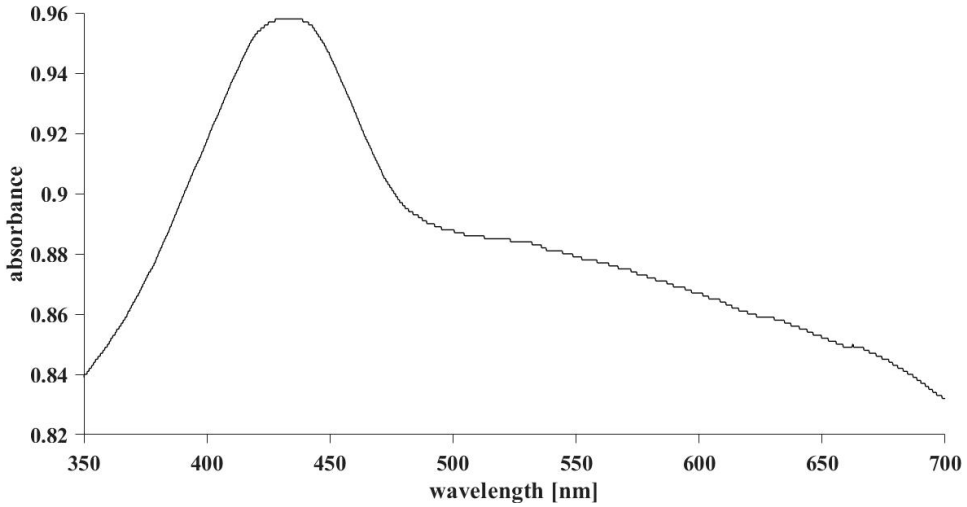

Figure 19. . UV-Vis of APTES magnetite nanoparticles functionalized with curcumin.

Route 2. In the second route curcumin has been involved in the synthesis process of MNPs aiming to graft them without the use of other molecules.

Two attempts were made employing the iron salts concentrations and following the steps of the classical MNPs synthesis but varying the way to dissolve curcumin. Figure 20 shows the FT-IR spectra of the nanoparticles obtained when the aqueous curcumin solution had a basic pH (black) or a neutral pH (green). In both cases the peak ascribable at the vibrational modes of Fe-O bonds is visible confirming the formation of MNPs. The peaks related to the C=O and aromatic C=C bonds of curcumin are also present. However, some difficulties occur during the sample preparation as not-dissolved curcumin tended to settle on the MNPs to be dried, so this can affect the obtained results.

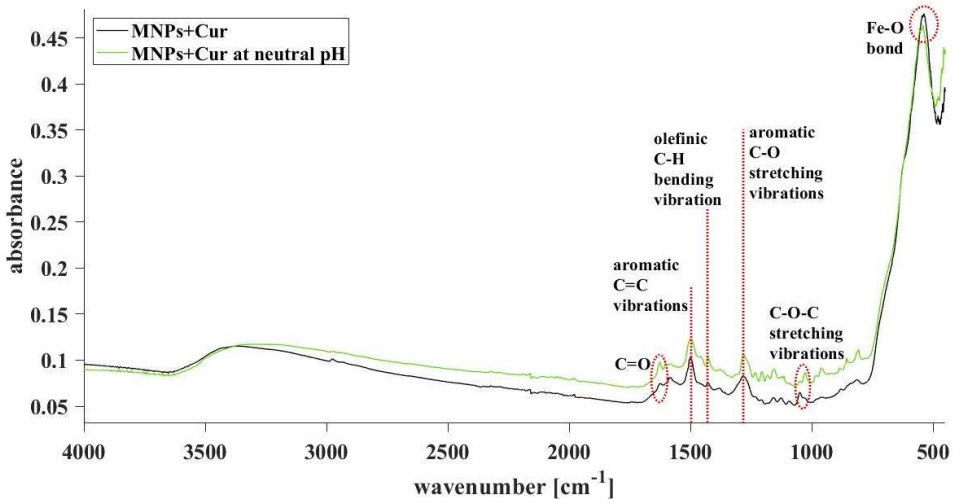

Figure 20. FT-IR spectra of magnetite nanoparticles synthesized using curcumin at basic pH (black) and neutral pH (green).

Another test has been conducted decreasing the iron salts concentration of an order of magnitude and dissolving curcumin in an alkaline aqueous solution. The FT-IR spectra reported in Figure 21 are related to the synthesis of magnetite nanoparticles without using curcumin (black) and the synthesis of magnetite nanoparticles involving curcumin (green). The effectiveness of the synthesis after the modification of the concentration parameter is verified as the characteristic peak that refers to the strong vibrational modes of Fe-O bonds is present. When curcumin take part to the synthesis it reacts with the other compounds as confirmed by the visible C=O and aromatic C=C bonds peaks, but magnetite is not formed because nanoparticles do not respond to the application of an external applied magnetic field. For this reason, the peak relative to the vibrational modes of Fe-O bonds observable in the spectra, may indicate the formation of other iron oxide compounds as curcumin is able to form strong complexes with metal ions, including Fe^{3+}.

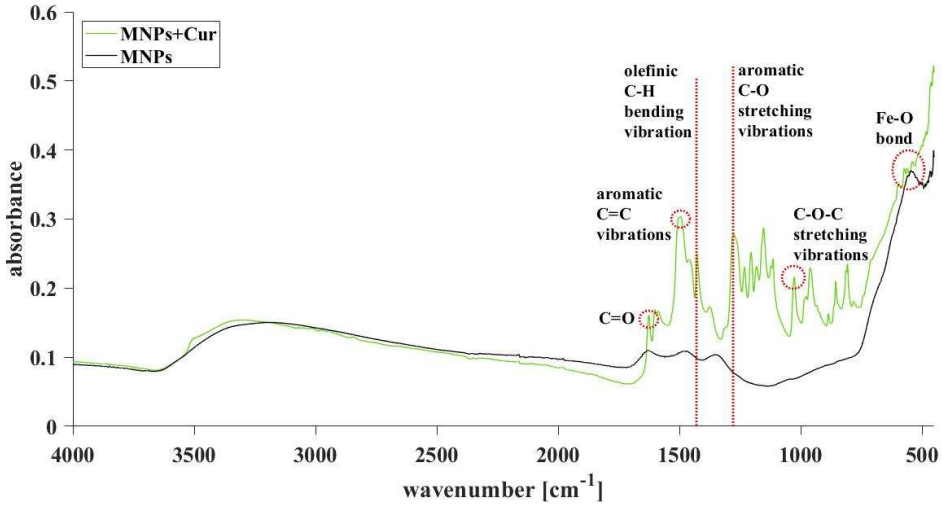

Figure 21. FT-IR spectra of magnetite nanoparticles (black) and curcumin functionalized magnetite nanoparticles (green).

From the characterization analysis it turned out that the direct functionalization of magnetite nanoparticles with curcumin (route 1) was unsuccessful, unlike the case of previous magnetite nanoparticles functionalization with APTES since the exposed NH_2 group allowed to bond curcumin.

Aiming to obtain a successful method to directly functionalize magnetite nanoparticles with curcumin, the results inherent to the nanoparticles synthesized via route 1 suggests that some parameters need to be varied, like a solvent type and a pH value that can enhance curcumin solubility since in the first attempt it appeared that curcumin remain not-dissolved affecting the final results while in the other case it prevented the formation of magnetite. However, as the previous functionalization of magnetite nanoparticles with APTES ensured the grafting of curcumin biomolecule, the route 2 synthesis have been subsequently repeated trying to conjugate these nanoparticles with AuNPs (discussed in detail in the following paragraph).

4.4 Gold-magnetite nanoparticles

After managing to employ curcumin as reducing and stabilizing agent for the synthesis of AuNPs and functionalizing agent in the synthesis of magnetite nanoparticles, the final tests of the experimental work concern the possibility to use curcumin as linking agent for the formation of hybrid gold-magnetite nanostructures. To achieve this goal, two different routes have been followed and the obtained nanostructures have been analysed through UV-Vis, FT-IR, and EDS.

Route 1. The starting point of the route 1 is the curcumin-mediated reduction of AuNPs, while the grafting of magnetite nanoparticles was performed in a later step. This route was repeated two times varying the gold nanoparticles synthesis method and the gold:magnetite solutions ratio.

In the first attempt, gold nanoparticles have been synthesized via route 1 (dissolving curcumin in aqueous NaOH solution) and magnetite nanoparticles previously synthesized were added in 2:1 ratio.
The UV-Vis analysis was performed at the end of each step showing that gold nanoparticles synthesis was successful (red curve) but after the magnetite nanoparticles addition the SPR absorbance peak was no more visible (black curve) (Figure 22), suggesting that after gold reduction curcumin was not able to bind with magnetite nanoparticles and curcumin gold nanoparticles have been removed during the washing steps.

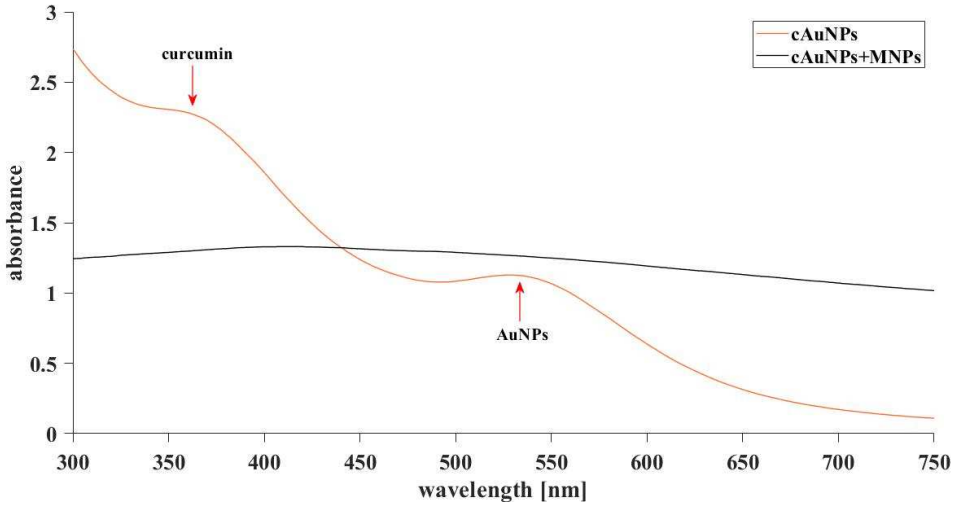

Figure 22. UV-Vis of gold nanoparticles (red) and gold-magnetite nanostructures (black).

Moreover, observing the FT-IR spectra in Figure 23 no differences can be seen between the one related to the magnetite nanoparticles and the other that refers to the gold-magnetite nanoparticles confirming the absence of curcumin on magnetite nanoparticles and the failure of the functionalization with curcumin gold nanoparticles.

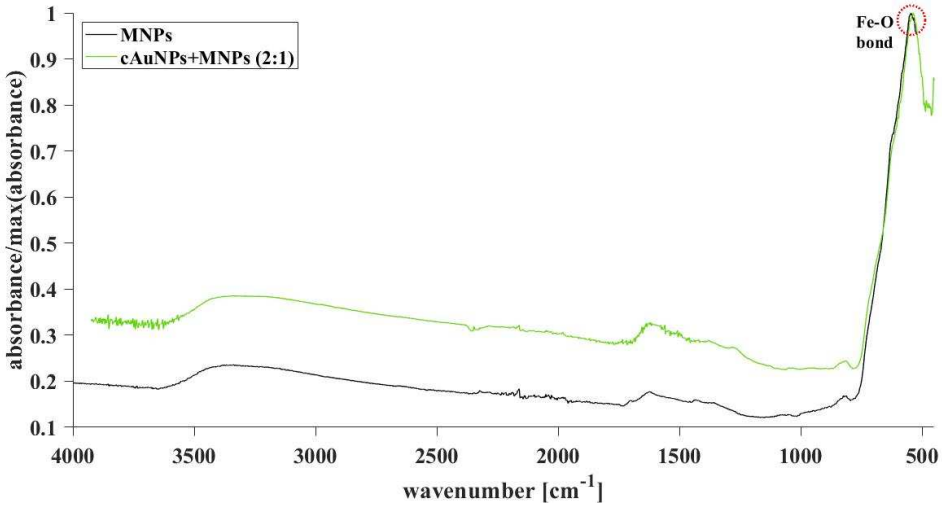

Figure 23. FT-IR spectra of magnetite nanoparticles (black) and gold-magnetite nanostructures (green).

This result is further confirmed by the chemical composition analysis as the presence of gold is not detected in the EDS spectrum unlike the components of magnetite, iron and

oxygen, whose peaks are easily visible in Figure 24. Carbon peak may be due to the grid.

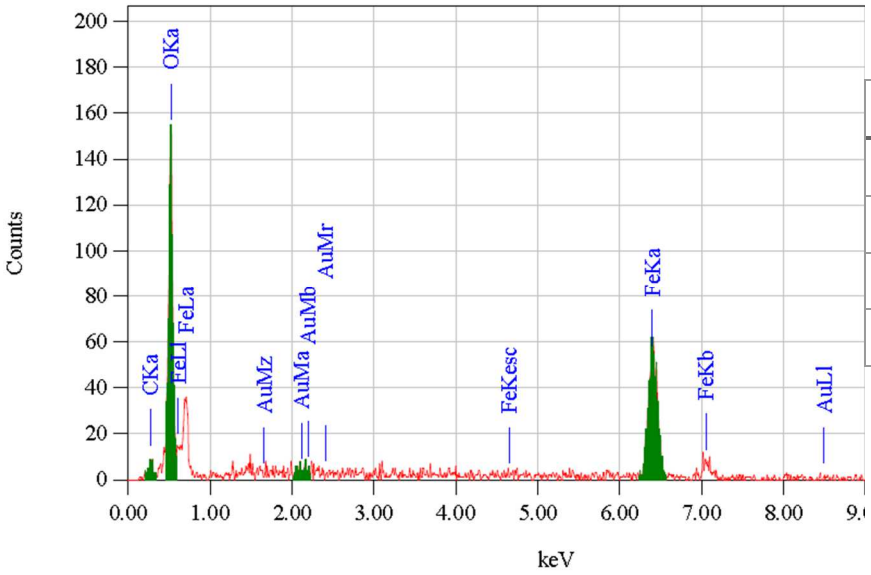

Element	Atom %
C	10.48
O	58.03
Fe	31.49
Au	ND

Figure 24. EDS analysis of gold-magnetite nanostructures (route 1, 2:1 ratio).

Hypothesizing that the gold nanoparticles quantity was too small compared to magnetite nanoparticles, this synthesis route was repeated halving the amount of magnetite nanoparticles solution (4:1 ratio). Also, gold nanoparticles have been synthesized via route 2 (that is bringing the pH value of curcumin aqueous solution at around 9.3 using K_2CO_3) before adding magnetite nanoparticles.

Also in this case the UV-Vis analysis was performed at the end of each step, the spectrum in Figure 25 ascertain the synthesis of gold nanoparticles but the SPR absorbance peak disappear after the magnetite nanoparticles addition suggesting that curcumin gold nanoparticles have been eliminated again during the washing steps.

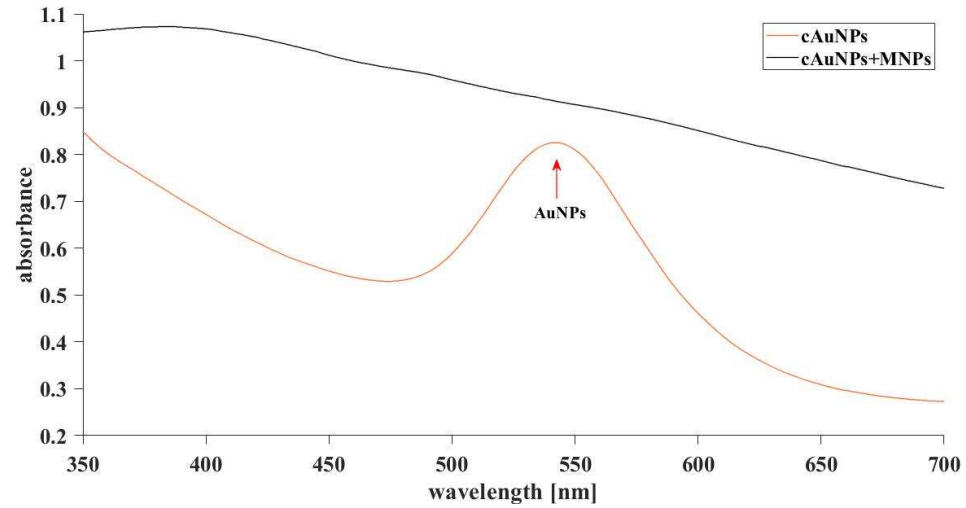

Figure 25. UV-Vis of gold nanoparticles (red) and gold-magnetite nanostructures (black).

Nevertheless, in the FT-IR spectrum (Figure 26) the main characteristic peaks of curcumin may be located indicating a possible grafting on the magnetite nanoparticles surface. As this is in contrast with the previous result, it can be hypothesized that that addition of magnetite nanoparticles can affect the interaction between curcumin and gold reduced ions leading to a break in their bond.

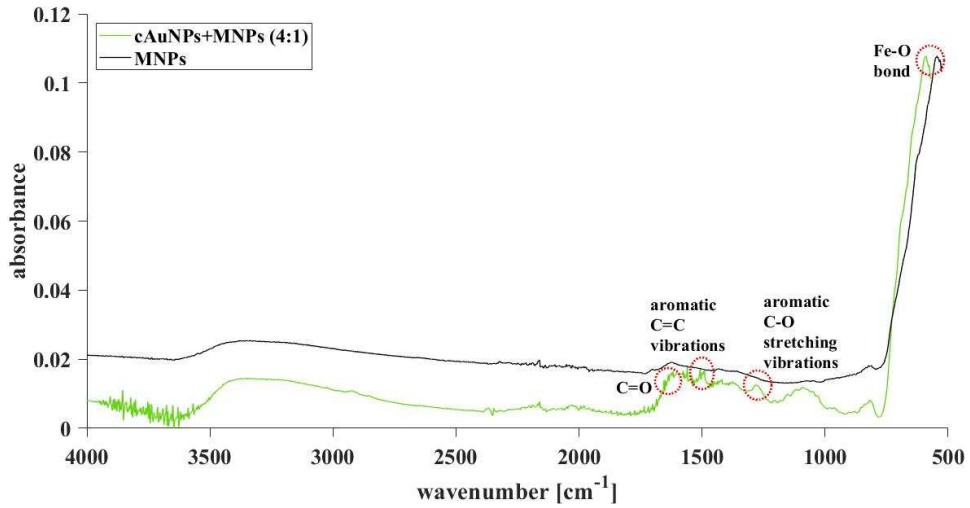

Figure 26. FT-IR spectra of magnetite nanoparticles (black) and gold-magnetite nanostructures (green).

Moreover, compared to the previous case, the EDS analysis (Figure 27) detected a very small amount of gold (1% compared to the percentage of Fe) even if it is lower than the instrument precision and is comparable to the percentage of other elements considered

to be impurities due to contaminations occurred during the synthesis and the sample preparation.

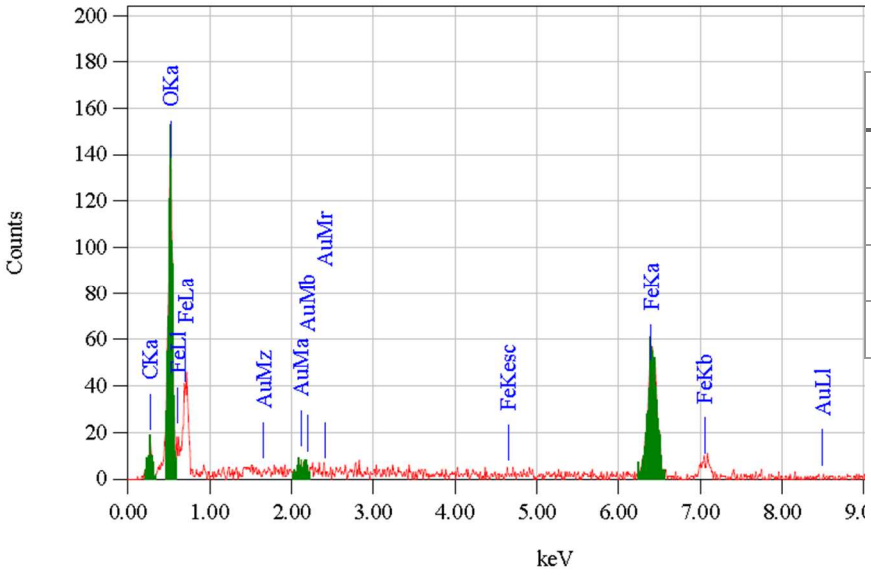

Element	Atom %
C	17.32
O	56.04
Fe	26.37
Au	0.27

Figure 27. EDS analysis of gold-magnetite nanostructures (route 1, 4:1 ratio).

Route 2. In this synthesis, magnetite nanoparticles were functionalized with APTES and curcumin with the aim to reduce gold ions directly on their surface to obtain hybrid nanostructures.

In the FT-IR spectrum detected after the gold nanoparticles reduction, the characteristic peaks of magnetite, APTES, and curcumin are still visible as evidenced in Figure 28, suggesting that the curcumin phenolic moiety interaction with NH_2 terminal groups of APTES is not influenced by the curcumin reduction of gold ions.

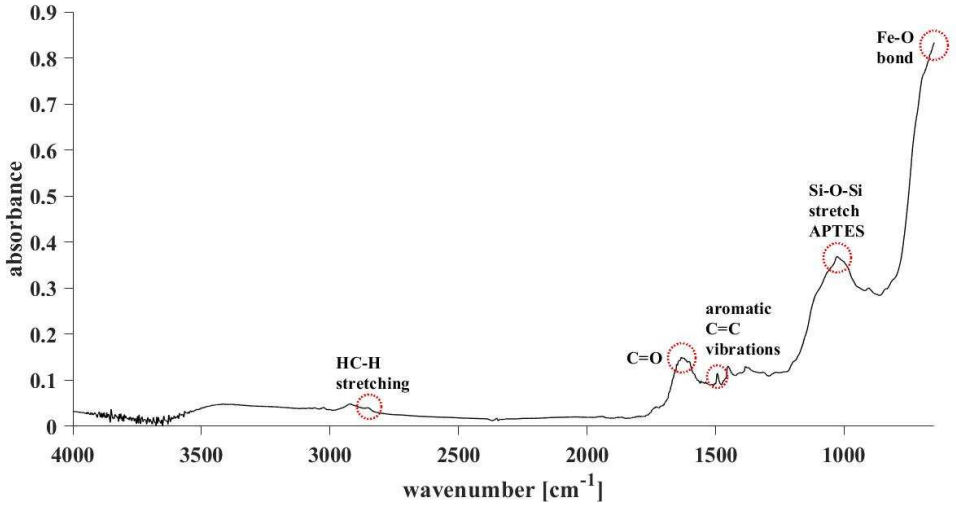

Figure 28. FT-IR spectrum of gold-magnetite nanostructures (route 2).

The UV-Vis analysis was performed to verify the successful synthesis of gold nanoparticles. The spectrum is reported in Figure 29 where it can be seen a broad band in which is possible to identify two peaks: the first at around 420 nm and the second at around 500 nm that may refers to curcumin and gold respectively. Consequently, it could be hypothesized that after curcumin binding with APTES functionalized magnetite nanoparticles there are still free reaction sites (O^- of the enolic moiety and of an aromatic ring) that can reduce gold ions.

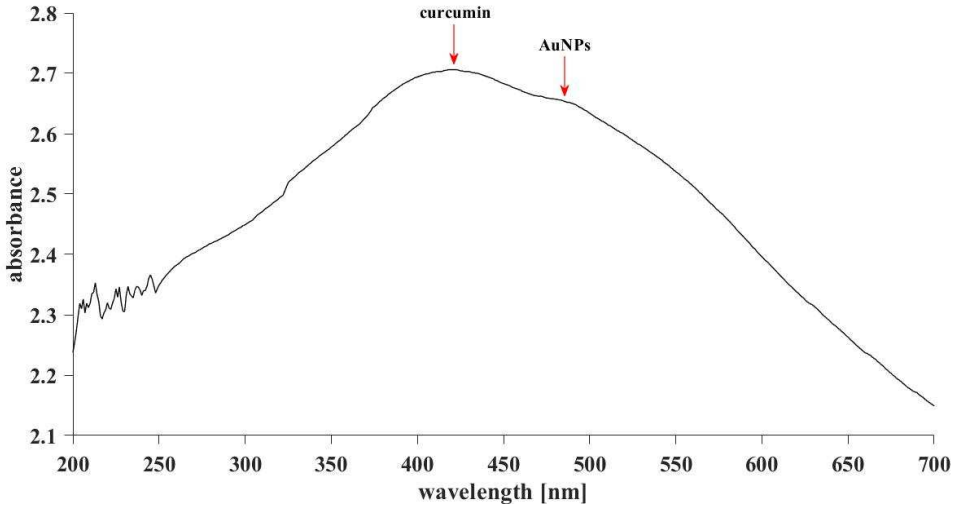

Figure 29. UV-Vis of gold-magnetite nanostructures (route 2).

A further confirmation to the presence of gold on this nanostructure is provided by the EDS spectrum (Figure 30) as its atom % increase compared to the precedent route, as well as its percentage (3,4%) related to the amount of iron. The main peaks are the ones related to oxygen and iron as they are the chemical components of magnetite nanoparticles, but also a silicon peak have been detected confirming the APTES functionalization. The carbon detection may be due to the grid.

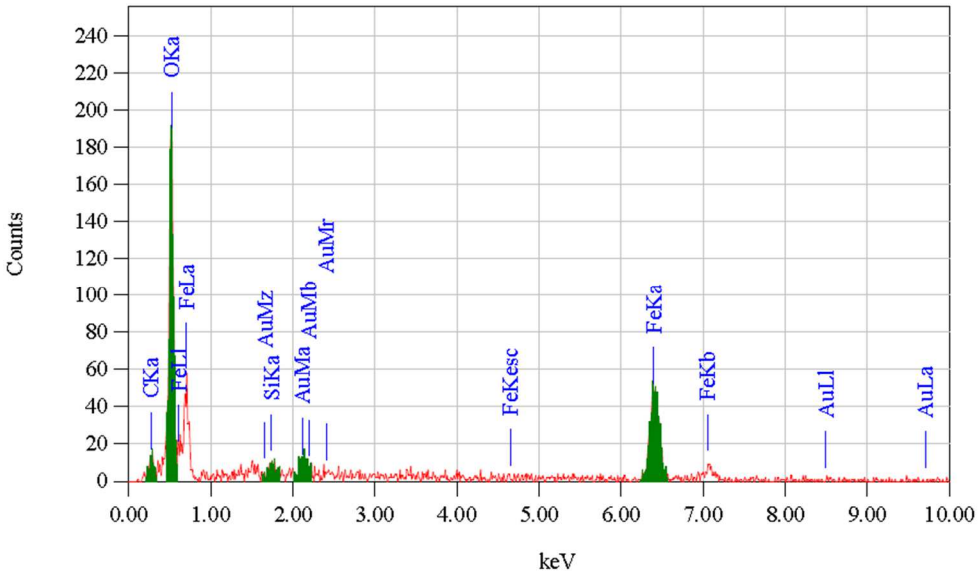

Element	Atom %
C	11.33
O	66
Fe	21.03
Au	0.74
Si	0.89

Figure 30. EDS analysis of gold-magnetite nanostructures (route 2).

The first attempt to bind naked magnetite nanoparticles with gold nanoparticles reduced and stabilized using curcumin biomolecule (route 1) proved to be unsuccessful as the presence of gold on the final nanostructures was not detected; after varying the gold:magnetite concentration ratio, some curcumin related peaks on the FT-IR spectrum can suggest an interaction between curcumin and magnetite nanoparticles but the characteristic gold absorbance peak, previously detected, was no more visible after mixing the two nanoparticles solution indicating another synthesis failure. Instead, the formation of conjugated gold-magnetite nanostructures via route 2 synthesis is confirmed by the analysis results, that showed the successful reduction gold ions by the action of curcumin grafted on APTES functionalized magnetite nanoparticles.

Chapter 5

Conclusions

The study and the analyses conducted during this work thesis had the purpose to develop a simple and eco-friendly synthesis process that involve the use of curcumin as novel biomolecule to produce hybrid nanostructures intended for biomedical applications.
Aiming to confer enhanced magnetic and optic properties to these hybrid nanostructures, the selected constituents are gold and magnetite nanoparticles. Thus, prior attempts have been made to verify the action of curcumin as reducing and stabilizing agent in the synthesis of gold nanoparticles and functionalizing biomolecule for the magnetite nanoparticles.

Two rapid single step methods for the synthesis of gold nanoparticles have been successfully carried out, confirming the action of curcumin as reducing and stabilizing agent about which studies have already been published in the literature. The optical properties of curcumin gold nanoparticles were ascertained through the UV-Vis analysis which highlighted the presence of the surface plasmon resonance related peak at 540 nm. However, the definition of a precise protocol is needed to make this green synthesis methods suitable for large scale production, as both resulted highly susceptible to environmental conditions.

The direct curcumin functionalization of magnetite nanoparticles during their synthesis via co-precipitation method failed, but the previous functionalization with APTES proved to be a good resolution that allowed to graft curcumin on their surface, as confirmed by the identification of their organic functional groups on the FT-IR spectra. Since APTES is biocompatible, its use does not represent a limitation for possible biomedical applications, according to this curcumin APTES functionalized magnetite nanoparticles have been chosen for the subsequent test concerning the hybrid nanostructures synthesis. Anyway, further attempts need to be conducted with the aim to obtain a curcumin magnetite nanoparticles functionalization without involving other

molecules varying synthesis parameters like the chemicals concentration or the solvent employed for curcumin dissolution.

Lastly, two different routes were pursued trying to create a unique nanostructure in which both gold and magnetite nanoparticles are present.
The first, that consists in using curcumin to reduce gold nanoparticles and later to link magnetite nanoparticles throughout reaction sites which may still be available, flopped as highlighted by the characterization analyses results, especially the EDS ones which revealed the absence of a significant gold atom percentage in the final nanostructures. In spite of this, other tests related to this synthesis route may be performed introducing a new step aimed at a previous functionalization of magnetite nanoparticles, that in this case where added to the curcumin gold nanoparticles suspension without modifying their surface.
In the other route the steps have been reversed, so curcumin was bonded to APTES functionalized magnetite nanoparticles followed by the reduction of gold nanoparticles directly on their surface. The second route can be promising based on what resulted from the characterization analysis. The EDS detected the presence of gold on the final nanostructures, besides that of magnetite constituent, as well as in the UV-Vis spectrum an absorbance peak is visible in the characteristic gold nanoparticles band. Also, the magnetic behaviour of the final nanostructures is confirmed by their response to an applied external magnetic field. Anyhow, further studies are needed to prove it is a successful synthesis method starting from characterization analyses aimed at observing the morphology of these hybrid nanostructures to confirm the gold nanoparticles reduction.

This project represents only a starting point as the final aim is the development of multifunctional nanostructures that can be employed as theranostic devices especially intended for cancer treatment, taking advantage of their magnetic and optical properties that allow to administrate a targeted photothermal therapy and the presence of curcumin that can act as therapeutic agent because of its multiple biological activities that confer to this biomolecule a potential antitumour action.

References

[1] "What Is Nanotechnology?," *nano.gov*. https://www.nano.gov/nanotech-101/what/definition (accessed Mar. 16, 2021).

[2] A. S. de Dios and M. E. Díaz-García, "Multifunctional nanoparticles: Analytical prospects," *Anal. Chim. Acta*, vol. 666, no. 1–2, pp. 1–22, 2010, doi: 10.1016/j.aca.2010.03.038.

[3] C. Daruich De Souza, B. Ribeiro Nogueira, and M. E. C. M. Rostelato, "Review of the methodologies used in the synthesis gold nanoparticles by chemical reduction," *J. Alloys Compd.*, vol. 798, pp. 714–740, 2019, doi: 10.1016/j.jallcom.2019.05.153.

[4] N. Sanvicens and M. P. Marco, "Multifunctional nanoparticles - properties and prospects for their use in human medicine," *Trends Biotechnol.*, vol. 26, no. 8, pp. 425–433, 2008, doi: 10.1016/j.tibtech.2008.04.005.

[5] C. Multari *et al.*, "Magnetoplasmonic nanoparticles for photothermal therapy," *Nanotechnology*, vol. 30, no. 25, pp. 1–201, 2019, doi: 10.1088/1361-6528/ab08f7.

[6] L. Hajba and A. Guttman, "The use of magnetic nanoparticles in cancer theranostics: Toward handheld diagnostic devices," *Biotechnol. Adv.*, vol. 34, no. 4, pp. 354–361, 2016, doi: 10.1016/j.biotechadv.2016.02.001.

[7] D. Kim, K. Shin, S. G. Kwon, and T. Hyeon, "Synthesis and Biomedical Applications of Multifunctional Nanoparticles," *Adv. Mater.*, vol. 30, no. 49, pp. 1–26, 2018, doi: 10.1002/adma.201802309.

[8] S. Fatemeh Shams, M. R. Ghazanfari, and C. Schmitz-Antoniak, "Magnetic-plasmonic heterodimer nanoparticles: Designing contemporarily features for emerging biomedical diagnosis and treatments," *Nanomaterials*, vol. 9, no. 1, 2019, doi: 10.3390/nano9010097.

[9] A. H. Lu, E. L. Salabas, and F. Schüth, "Magnetic nanoparticles: Synthesis, protection, functionalization, and application," *Angew. Chemie - Int. Ed.*, vol. 46,

no. 8, pp. 1222–1244, 2007, doi: 10.1002/anie.200602866.

[10] L. Mohammed, H. G. Gomaa, D. Ragab, and J. Zhu, "Magnetic nanoparticles for environmental and biomedical applications: A review," *Particuology*, vol. 30, pp. 1–14, 2017, doi: 10.1016/j.partic.2016.06.001.

[11] G. Goya, V. Grazu, and M. Ibarra, "Magnetic Nanoparticles for Cancer Therapy," *Curr. Nanosci.*, vol. 4, pp. 1–16, 2008, doi: 10.2174/157341308783591861.

[12] S. Satanassi, "Teranostica: diagnosi e cura attraverso nanoparticelle."

[13] S. Gul, S. B. Khan, I. U. Rehman, M. A. Khan, and M. I. Khan, "A Comprehensive Review of Magnetic Nanomaterials Modern Day Theranostics," *Front. Mater.*, vol. 6, no. July, pp. 1–15, 2019, doi: 10.3389/fmats.2019.00179.

[14] P. Srivastava, P. K. Sharma, A. Muheem, and M. H. Warsi, "Magnetic Nanoparticles: A Review on Stratagems of Fabrication an d its Biomedical Applications," *Recent Pat. Drug Deliv. Formul.*, vol. 11, no. 2, 2017, doi: 10.2174/1872211311666170328150747.

[15] W. Wu, Z. Wu, T. Yu, C. Jiang, and W. S. Kim, "Recent progress on magnetic iron oxide nanoparticles: Synthesis, surface functional strategies and biomedical applications," *Sci. Technol. Adv. Mater.*, vol. 16, no. 2, 2015, doi: 10.1088/1468-6996/16/2/023501.

[16] A. Pariti, "Gold Magnetite Nanoparticle Biomolecule Conjugates : Synthesis , Properties and Toxicity Studies," 2014.

[17] L. Maldonado-Camargo, I. Torres-Díaz, M. Hernández, and C. Rinaldi, "Estimating the contribution of Brownian and N´eel relaxation in a magnetic fluid through dynamic magnetic susceptibility measurements," *J. Magn. Magn. Mater.*, 2016, doi: 10.1016/j.jmmm.2016.03.087.

[18] C. C. Berry, "Progress in functionalization of magnetic nanoparticles for applications in biomedicine," *J. Phys. D. Appl. Phys.*, vol. 42, no. 22, 2009, doi: 10.1088/0022-3727/42/22/224003.

[19] A. K. Gupta and M. Gupta, "Synthesis and surface engineering of iron oxide

nanoparticles for biomedical applications," *Biomaterials*, vol. 26, no. 18, pp. 3995–4021, 2005, doi: 10.1016/j.biomaterials.2004.10.012.

[20] K. Hola, Z. Markova, G. Zoppellaro, J. Tucek, and R. Zboril, "Tailored functionalization of iron oxide nanoparticles for MRI, drug delivery, magnetic separation and immobilization of biosubstances," *Biotechnol. Adv.*, vol. 33, no. 6, pp. 1162–1176, 2015, doi: 10.1016/j.biotechadv.2015.02.003.

[21] M. Sengani, A. M. Grumezescu, and V. D. Rajeswari, "Recent trends and methodologies in gold nanoparticle synthesis – A prospective review on drug delivery aspect," *OpenNano*, vol. 2, no. July, pp. 37–46, 2017, doi: 10.1016/j.onano.2017.07.001.

[22] M. Kim, J. H. Lee, and J. M. Nam, "Plasmonic Photothermal Nanoparticles for Biomedical Applications," *Adv. Sci.*, vol. 6, no. 17, 2019, doi: 10.1002/advs.201900471.

[23] M. Manca, "Sintesi , caratterizzazione e studio delle proprietà ottiche nonlineari di array 2D di nanostrutture plasmoniche," 2015.

[24] D. K. Kirui, D. A. Rey, and C. A. Batt, "Gold hybrid nanoparticles for targeted phototherapy and cancer imaging," *Nanotechnology*, vol. 21, no. 10, 2010, doi: 10.1088/0957-4484/21/10/105105.

[25] E. K. Fodjo, K. M. Gabriel, B. Y. Serge, D. Li, C. Kong, and A. Trokourey, "Selective synthesis of Fe3O4AuxAgy nanomaterials and their potential applications in catalysis and nanomedicine," *Chem. Cent. J.*, vol. 11, no. 1, pp. 1–9, 2017, doi: 10.1186/s13065-017-0288-y.

[26] M. Temelie, R. C. Popescu, D. Cocioaba, B. S. Vasile, and D. Savu, "Biocompatibility study of magnetite nanoparticle synthesized using a Green method," *Rom. J. Phys.*, vol. 63, no. 7–8, pp. 1–13, 2018.

[27] S. Ahmed, Annu, S. Ikram, and S. Yudha, "Biosynthesis of gold nanoparticles: A green approach," *J. Photochem. Photobiol. B Biol.*, vol. 161, pp. 141–153, 2016, doi: 10.1016/j.jphotobiol.2016.04.034.

[28] M. Shah, D. Fawcett, S. Sharma, S. K. Tripathy, and G. E. J. Poinern, *Green*

synthesis of metallic nanoparticles via biological entities, vol. 8, no. 11. 2015.

[29] S. Menon, R. S., and V. K. S., "A review on biogenic synthesis of gold nanoparticles, characterization, and its applications," *Resour. Technol.*, vol. 3, no. 4, pp. 516–527, 2017, doi: 10.1016/j.reffit.2017.08.002.

[30] J. Jeevanandam, Y. S. Chan, and M. K. Danquah, "Biosynthesis of Metal and Metal Oxide Nanoparticles," *ChemBioEng Rev.*, vol. 3, no. 2, pp. 55–67, 2016, doi: 10.1002/cben.201500018.

[31] W. Marimon-Bolivar and N. Toussaint-Jimenez, "A review on green synthesis of magnetic nanoparticles (magnetite) for environmental applications," *2019 Congr. Int. Innov. y Tendencias en Ing. CONIITI 2019 - Conf. Proc.*, 2019, doi: 10.1109/CONIITI48476.2019.8960849.

[32] S. Venkateswarlu, B. Natesh Kumar, C. H. Prasad, P. Venkateswarlu, and N. V. V. Jyothi, "Bio-inspired green synthesis of Fe3O4 spherical magnetic nanoparticles using Syzygium cumini seed extract," *Phys. B Condens. Matter*, vol. 449, pp. 67–71, 2014, doi: 10.1016/j.physb.2014.04.031.

[33] A. M. Awwad and N. M. Salem, "A Green and Facile Approach for Synthesis of Magnetite Nanoparticles," *Nanosci. Nanotechnol.*, vol. 2, no. 6, pp. 208–213, 2013, doi: 10.5923/j.nn.20120206.09.

[34] A. K. Mittal, J. Bhaumik, S. Kumar, and U. C. Banerjee, "Biosynthesis of silver nanoparticles: Elucidation of prospective mechanism and therapeutic potential," *J. Colloid Interface Sci.*, vol. 415, pp. 39–47, 2014, doi: 10.1016/j.jcis.2013.10.018.

[35] D. Raghunandan, M. D. Bedre, S. Basavaraja, B. Sawle, S. Y. Manjunath, and A. Venkataraman, "Rapid biosynthesis of irregular shaped gold nanoparticles from macerated aqueous extracellular dried clove buds (Syzygium aromaticum) solution," *Colloids Surfaces B Biointerfaces*, vol. 79, no. 1, pp. 235–240, 2010, doi: 10.1016/j.colsurfb.2010.04.003.

[36] K. Krishnaswamy, H. Vali, and V. Orsat, "Value-adding to grape waste: Green synthesis of gold nanoparticles," *J. Food Eng.*, vol. 142, no. June, pp. 210–220, 2014, doi: 10.1016/j.jfoodeng.2014.06.014.

[37] N. Basavegowda, A. Idhayadhulla, and Y. R. Lee, “Phyto-synthesis of gold nanoparticles using fruit extract of Hovenia dulcis and their biological activities,” *Ind. Crops Prod.*, vol. 52, pp. 745–751, 2014, doi: 10.1016/j.indcrop.2013.12.006.

[38] P. C. Nagajyothi, K. D. Lee, and T. V. M. Sreekanth, “Biogenic synthesis of gold nanoparticles (quasi-spherical, triangle, and hexagonal) using lonicera japonica flower extract and its antimicrobial activity,” *Synth. React. Inorganic, Met. Nano-Metal Chem.*, vol. 44, no. 7, pp. 1011–1018, 2014, doi: 10.1080/15533174.2013.797456.

[39] P. Velmurugan *et al.*, “Phyto-crystallization of silver and gold by Erigeron annuus (L.) Pers flower extract and catalytic potential of synthesized and commercial nano silver immobilized on sodium alginate hydrogel,” *J. Saudi Chem. Soc.*, vol. 20, no. 3, pp. 313–320, 2016, doi: 10.1016/j.jscs.2014.09.004.

[40] A. Rai, M. Chaudhary, A. Ahmad, S. Bhargava, and M. Sastry, “Synthesis of triangular Au core-Ag shell nanoparticles,” *Mater. Res. Bull.*, vol. 42, no. 7, pp. 1212–1220, 2007, doi: 10.1016/j.materresbull.2006.10.019.

[41] K. Gopinath, S. Gowri, V. Karthika, and A. Arumugam, “Green synthesis of gold nanoparticles from fruit extract of Terminalia arjuna, for the enhanced seed germination activity of Gloriosa superba,” *J. Nanostructure Chem.*, vol. 4, no. 3, 2014, doi: 10.1007/s40097-014-0115-0.

[42] S. S. Shankar, A. Rai, A. Ahmad, and M. Sastry, “Rapid synthesis of Au, Ag, and bimetallic Au core-Ag shell nanoparticles using Neem (Azadirachta indica) leaf broth,” *J. Colloid Interface Sci.*, vol. 275, no. 2, pp. 496–502, 2004, doi: 10.1016/j.jcis.2004.03.003.

[43] Y. Nangia, N. Wangoo, N. Goyal, G. Shekhawat, and C. R. Suri, “A novel bacterial isolate Stenotrophomonas maltophilia as living factory for synthesis of gold nanoparticles,” *Microb. Cell Fact.*, vol. 8, no. 1, pp. 1–7, 2009, doi: 10.1186/1475-2859-8-39.

[44] Z. Wang, H. Zhu, X. Wang, F. Yang, and X. Yang, “One-pot green synthesis of biocompatible arginine-stabilized magnetic nanoparticles,” *Nanotechnology*, vol.

20, no. 46, 2009, doi: 10.1088/0957-4484/20/46/465606.

[45] A. Demir, R. Topkaya, and A. Baykal, “Green synthesis of superparamagnetic Fe3O4 nanoparticles with maltose: Its magnetic investigation,” *Polyhedron*, vol. 65, pp. 282–287, 2013, doi: 10.1016/j.poly.2013.08.041.

[46] J. Kasthuri, S. Veerapandian, and N. Rajendiran, “Biological synthesis of silver and gold nanoparticles using apiin as reducing agent,” *Colloids Surfaces B Biointerfaces*, vol. 68, no. 1, pp. 55–60, 2009, doi: 10.1016/j.colsurfb.2008.09.021.

[47] W. Wang, Q. Chen, C. Jiang, D. Yang, X. Liu, and S. Xu, “One-step synthesis of biocompatible gold nanoparticles using gallic acid in the presence of poly-(N-vinyl-2-pyrrolidone),” *Colloids Surfaces A Physicochem. Eng. Asp.*, vol. 301, no. 1–3, pp. 73–79, 2007, doi: 10.1016/j.colsurfa.2006.12.037.

[48] K. I. Priyadarsini, “The chemistry of curcumin: From extraction to therapeutic agent,” *Molecules*, vol. 19, no. 12, pp. 20091–20112, 2014, doi: 10.3390/molecules191220091.

[49] R. Appiah-Opong, J. N. M. Commandeur, B. van Vugt-Lussenburg, and N. P. E. Vermeulen, “Inhibition of human recombinant cytochrome P450s by curcumin and curcumin decomposition products,” *Toxicology*, vol. 235, no. 1–2, pp. 83–91, 2007, doi: 10.1016/j.tox.2007.03.007.

[50] P. Kumavat, S. D.; Chaudhari, Y. S.; Borole, P.; Mishra, P.; Shenghani, K.; Duvvuri, “Degradation studies of curcumin,” *Int. J. Pharm. Rev. Res.*, vol. 3, no. 1, pp. 50–55, 2013.

[51] S. V. Jovanovic, S. Steenken, C. W. Boone, and M. G. Simic, “H-atom transfer is a preferred antioxidant mechanism of curcumin,” *J. Am. Chem. Soc.*, vol. 121, no. 41, pp. 9677–9681, 1999, doi: 10.1021/ja991446m.

[52] B. Zheng and D. J. McClements, “Formulation of more efficacious curcumin delivery systems using colloid science: Enhanced solubility, stability, and bioavailability,” *Molecules*, vol. 25, no. 12, pp. 1–25, 2020, doi: 10.3390/molecules25122791.

[53] B. Salehi *et al.*, “Curcumin’s Nanomedicine Formulations for Therapeutic Application in Neurological Diseases,” *J. Clin. Med.*, vol. 9, no. 2, p. 430, 2020, doi: 10.3390/jcm9020430.

[54] R. Rahimnia, Z. Salehi, M. S. Ardestani, and H. Doosthoseini, “SPION conjugated curcumin nano-imaging probe: Synthesis and bio-physical evaluation,” *Iran. J. Pharm. Res.*, vol. 18, no. 1, pp. 183–197, 2019, doi: 10.22037/ijpr.2019.2331.

[55] M. M. Yallapu *et al.*, “Curcumin-loaded magnetic nanoparticles for breast cancer therapeutics and imaging applications,” *Int. J. Nanomedicine*, vol. 7, pp. 1761–1779, 2012, doi: 10.2147/IJN.S29290.

[56] R. Bhandari, P. Gupta, T. Dziubla, and J. Z. Hilt, “Single step synthesis, characterization and applications of curcumin functionalized iron oxide magnetic nanoparticles,” *Mater. Sci. Eng. C*, vol. 67, pp. 59–64, 2016, doi: 10.1016/j.msec.2016.04.093.

[57] X. N. Pham, T. P. Nguyen, T. N. Pham, T. T. N. Tran, and T. V. T. Tran, “Synthesis and characterization of chitosan-coated magnetite nanoparticles and their application in curcumin drug delivery,” *Adv. Nat. Sci. Nanosci. Nanotechnol.*, vol. 7, no. 4, 2016, doi: 10.1088/2043-6262/7/4/045010.

[58] M. Qi *et al.*, “Superparamagnetic Fe3O4 nanoparticles: Synthesis by a solvothermal process and functionalization for a magnetic targeted curcumin delivery system,” *New J. Chem.*, vol. 40, no. 5, pp. 4480–4491, 2016, doi: 10.1039/c5nj02441b.

[59] L. D. Tran *et al.*, “Nanosized magnetofluorescent Fe3O4-curcumin conjugate for multimodal monitoring and drug targeting,” *Colloids Surfaces A Physicochem. Eng. Asp.*, vol. 371, no. 1–3, pp. 104–112, 2010, doi: 10.1016/j.colsurfa.2010.09.011.

[60] H. Nosrati, N. Sefidi, A. Sharafi, H. Danafar, and H. Kheiri Manjili, “Bovine Serum Albumin (BSA) coated iron oxide magnetic nanoparticles as biocompatible carriers for curcumin-anticancer drug,” *Bioorg. Chem.*, vol. 76, pp. 501–509, 2018, doi: 10.1016/j.bioorg.2017.12.033.

[61] C. Sreelakshmi, N. Goel, K. K. R. Datta, A. Addlagatta, R. Ummanni, and B. V. S. Reddy, "Green synthesis of curcumin capped gold nanoparticles and evaluation of their cytotoxicity," *Nanosci. Nanotechnol. Lett.*, vol. 5, no. 12, pp. 1258–1265, 2013, doi: 10.1166/nnl.2013.1678.

[62] F. Abdulwahab, F. Z. Henari, S. Cassidy, and K. Winser, "Synthesis of Au, Ag, Curcumin Au/Ag, and Au-Ag Nanoparticles and Their Nonlinear Refractive Index Properties," *J. Nanomater.*, vol. 2016, 2016, doi: 10.1155/2016/5356404.

[63] K. Sindhu, A. Rajaram, K. J. Sreeram, and R. Rajaram, "Curcumin conjugated gold nanoparticle synthesis and its biocompatibility," *RSC Adv.*, vol. 4, no. 4, pp. 1808–1818, 2014, doi: 10.1039/c3ra45345f.

[64] S. Nambiar, E. Osei, A. Fleck, J. Darko, A. J. Mutsaers, and S. Wettig, "Synthesis of curcumin-functionalized gold nanoparticles and cytotoxicity studies in human prostate cancer cell line," *Appl. Nanosci.*, vol. 8, no. 3, pp. 347–357, 2018, doi: 10.1007/s13204-018-0728-6.

[65] E. Shaabani, S. M. Amini, S. Kharrazi, and R. Tajerian, "Curcumin coated gold nanoparticles: synthesis, characterization, cytotoxicity, antioxidant activity and its comparison with citrate coated gold nanoparticles," vol. 4, no. 2, pp. 115–125, 2017, doi: 10.22038/nmj.2017.21506.1227.

[66] D. K. Singh, R. Jagannathan, P. Khandelwal, P. M. Abraham, and P. Poddar, "In situ synthesis and surface functionalization of gold nanoparticles with curcumin and their antioxidant properties: An experimental and density functional theory investigation," *Nanoscale*, vol. 5, no. 5, pp. 1882–1893, 2013, doi: 10.1039/c2nr33776b.

[67] S. Sundar, R. Mariappan, and S. Piraman, "Synthesis and characterization of amine modified magnetite nanoparticles as carriers of curcumin-anticancer drug," *Powder Technol.*, vol. 266, pp. 321–328, 2014, doi: 10.1016/j.powtec.2014.06.033.

[68] S. Villa, P. Riani, F. Locardi, and F. Canepa, "Functionalization of Fe3O4 NPs by silanization: Use of amine (APTES) and thiol (MPTMS) silanes and their physical characterization," *Materials (Basel).*, vol. 9, no. 10, 2016, doi:

10.3390/ma9100826.

[69] Nandiyanto *et al.*, "Extraction of Curcumin Pigment from Indonesian Local Turmeric with Its Infrared Spectra and Thermal Decomposition Properties," *J. Phys. Conf. Ser.*, vol. 755, no. 1, 2016, doi: 10.1088/1742-6596/755/1/011001.

[70] Wasatchphotonics.com, "Authentication of Turmeric with UV-VIS." https://wasatchphotonics.com/applications/turmeric-authentication-uv-vis/ (accessed Mar. 17, 2021).

[71] C. D. dos Santos, T. B. Henrique, P. C. B. Pacheco, F. M. Regina, and C. L. Coronato, "PEGylated curcumin with gold nanoparticles: Antimicrobial agent evaluation," *World Congr. Recent Adv. Nanotechnol.*, vol. 3, 2016, doi: 10.11159/nddte16.114.